Chapter 2

Synthesis, Characterization and Study of extended iso-indigo based donor-acceptor conjugated polymers

Table of contents

Introduction **34**

Results and discussion **42**

Synthesis of monomers and polymers 42

Molecular weight and thermal properties of polymers 44

Photophysical properties of monomers 46

Photo physical properties of polymers 47

Electrochemical properties of monomers 48

Electrochemical properties of polymers 49

Computational studies 52

X-ray diffraction studies of polymers 54

Space Charge Limited Current (SCLC) measurement of polymers 54

Conclusion **57**

Experimental procedures **58**

General procedure 58

Synthesis of 5-bromo-1-tetradecylindolin-2-one 58

Synthesis of 2,5-bis(hydroxymethyl)benzene-1,4-dialdehyde 59

Synthesis of monomers 61

Synthesis of (3Z,3'Z)-3,3'-(1,4-phenylenebis(methaneylylidene)) bis(5-bromo-1-tetradecylindolin-2-one) **(TIIG)** 61

Synthesis of (3Z,3'Z)-3,3'-((2,5-bis(dodecyloxy)-1,4-phenylene)bis(methaneylylidene)) bis(5-bromo-1-tetradecylindolin-2-one) **(DAB)** 62

Synthesis of (3Z,3'Z)-3,3'-(thiophene-2,5-diylbis(methaneylylidene)bis(5-bromo-1-tetradecylindolin-2-one) **(THP)** 62

Synthesis of polymers 63

General procedure for synthesis of iso-indigo based polymers **TIIG-P**, **DAB-P** and **THP-P** 63

Spectral data **65**

References **79**

Introduction

In recent years, there has been significant research and development in the field of conjugated polymers for various optoelectronic applications, including organic electronic devices like organic light-emitting diodes (OLEDs), organic field effect transistors (OFETs) and organic photovoltaics (OPVs).[1,2] Conjugated polymers offer several advantages in these applications due to their unique electronic and optical properties.[3,4] Conjugated polymers can have their electronic properties tuned by modifying the chemical structure. This allows researchers to design materials with specific energy levels suited for different device application such as OLEDs, OFETs, and OPVs.[5,6] Conjugated polymers can be solution-processed, allowing for the fabrication of flexible and low-cost electronic devices. This feature is particularly advantageous for wearable electronics and flexible displays.[7–9]

Organic conjugated molecules and polymers provide the basis for many desirable properties of optoelectronic devices, including low-cost production, flexibility, lightweight, and ease of usage over large surface areas.[10] Donor-acceptor (D-A) conjugated polymers have attracted a lot of attention recently as one of the most significant classes of organic semiconductor materials because of their outstanding performance in organic optoelectronic devices and their versatility in allowing the semiconducting properties to be tailored to specific structures.[11] Donor-acceptor conjugated polymers have demonstrated excellent performance in various organic optoelectronic devices, including organic photovoltaics (solar cells), OLEDs and OFETs.[12,13] They can efficiently convert light into electricity, emit light, or modulate electrical current. The chemical structure of donor-acceptor conjugated polymers can be finely tuned to control their electronic properties, such as bandgap, charge mobility, and energy levels.[14] This tunability enables the design of materials optimized for specific applications.[15]

A large number of electron-donating building blocks for the D-A-type conjugated polymers have been studied extensively, such as 2,2´-bithiophene,[10] thieno[3,2-*b*]thiophene,[16] 9-arylidene-9*H*-fluorene,[12] 9*H*-carbazole,[13] 3,7-dialkyltetrathienoacence,[14] 4*H*-cyclopenta[2,1-*b*:3,4-*b*´]dithiophene,[17] *N*-alkyl dithieno[3,2-*b*:2´,3´-*d*]pyrrole,[18] fused aryldipyrroles,[19] benzo[1,2-*b*:4,5-*b*´]dithiophene,[20] 4,9-dihydro-*s*-indaceno[1,2-*b*:5,6-*b*´]dithiophene,[21] diindeno[1,2-

b:2´,1´-*d*]thiophene,[22]dithieno[2,3-*d*:2´,3´-*d*]benzo[1,2-*b*:4,5-*b*´]dithiophene,[23] dithienocyclopentathieno[3,2-*b*]thiophene,[24] tetraalkylthieno [3´,2´:6,7][1] benzothieno[3,2-*b*]thieno[3,2-*g*][1]benzothiophene[25]. On the other hand, the progress in the development of electron-withdrawing building blocks is very less compared to that of electron-donating building blocks. Most frequently used electron-withdrawing units include 2,1,3-benzothiadiazole,[26] *N*-heteroacenes,[27] alkyl carbonyl-substituted thieno[3,4-*b*]thiophene,[28] naphtho[1,2-*c*:5,6-*c*]bis[1,2,5]thiadiazole,[29] thiazolo[5,4-*d*]thiazole,[15] and lactam- and imide-based acceptors. Imide-based acceptors such as naphthalene diimide,[30] perylene diimide,[31] tetraazabenzodifluoranthene diimide[32] and lactam-based acceptors such as diketopyrrolopyrrole (DPP),[33] indigo,[34] isoindigo,[35] benzodipyrrolidone,[36] dihydropyrroloindoledione,[37] indophenine,[38] thiophene-*S*,*S*-dioxidized indophenine,[39] and fused bis-isatins[40] have gathered significant attention.

Isoindigo is a synthetic organic compound that is derived from indigo, a natural pigment found in plants, particularly in the leaves of the indigo plant (*Indigofera tinctoria*) and some other species.[41] While isoindigo itself is not typically found in nature, it can be synthesized from indigo through chemical processes.[42] In the context of organic electronics and materials science, isoindigo and its derivatives have gained attention due to their electron-deficient nature. Electron-deficient compounds are often used as acceptor materials in organic photovoltaics and organic semiconductor devices, where they can form donor-acceptor (D-A) type copolymers or blends with electron-rich donor materials.[43] The electron-deficient nature of isoindigo derivatives makes them excellent candidates for accepting electrons from donor materials, which leads to efficient charge separation and transport in these copolymers. This is crucial for the performance of organic solar cells and OFETs. When incorporated into D-A-type copolymers, iso-indigo-based materials have been shown to exhibit excellent semiconducting properties, such as high charge mobility and good photovoltaic performance.[44]

Modifying the structure and electronic properties of iso-indigo is a common strategy in the field of organic chemistry and materials science. Two commonly applied strategies for such modifications are terminal modification and centre modification.

Terminal Modification: In terminal modification, the benzene rings at the ends of the isoindigo molecule are replaced with other conjugated units. This strategy can lead to

several changes in the properties of isoindigo-based compounds. The few such changes in properties are described below.

Tuning optical properties: Terminal modifications can influence the absorption and emission spectra of isoindigo-based materials. For example, the absorption and emission wavelengths can be shifted by replacing the terminal benzene rings with different aromatic groups, which is important for applications in organic electronics and photovoltaics.

Modulating solubility: Terminal modifications can also impact the solubility of isoindigo-based compounds in various solvents. This is crucial for solution-based processing methods used in device fabrication.

Changing HOMO-LUMO gap: Altering the terminal groups can affect the energy levels of the highest occupied molecular orbital (HOMO) and the lowest unoccupied molecular orbital (LUMO), which can in turn, impact the electronic properties and charge transport characteristics.

Enhancing packing and crystallinity: Modifying the terminal groups can optimize the molecular packing in solid-state materials, which potentially improving charge transport properties.

Centre Modification: Centre modification involves introducing conjugated units into the central part of the isoindigo molecule. This strategy is often employed to increase the effective conjugated length of isoindigo and avoid steric hindrance that might occur with terminal modifications. Key aspects of centre modification are mentioned below.

Extending conjugation: By inserting additional conjugated units into the central core of isoindigo, the effective conjugation length of the molecule can increase. This can result in enhanced electronic delocalization and consequently, altered electronic properties.

Reduction of steric hindrance: Centre modifications can reduce steric hindrance that may occur with larger or bulkier terminal substituents. This allows for more efficient packing in solid-state materials which improved the charge transportation.

Control over band gap: The introduction of specific conjugated units in the centre can allow for precise control over the band gap of isoindigo-based materials, which is important for tailoring their electronic properties for specific applications.

Enhanced charge mobility: Introduction of large conjugated system in the centre can improved charge mobility in the resultant organic electronic devices.

Both terminal and centre modifications are valuable strategies for tailoring the properties of isoindigo-based materials to suit various applications, including OPVs, OFETs, and OLEDs. The choice of modification strategy depends on the desired electronic and structural characteristics needed for a specific application.

The synthesis of π-extended isoindigo derivatives by inserting conjugated units into the central part of isoindigo is an important strategy in organic chemistry. This approach enhances the molecular planarity of isoindigo-based compounds, leading to several advantageous properties, including improved carrier mobility and effective spectral absorption. These modified isoindigo-based compounds have the potential to find applications in various organic electronic devices, particularly in the development of high-performance organic semiconductors and solar cells.[45,46]

Ting *et al.*[47] reported isoindigo-based polymer using 6-bromoisatin. Through intramolecular hydrogen bonding, the newly created electron-deficient PPV derivative "locked" the polymer backbone, giving it exceptional properties. Higher electron mobilities up to 1.1 $cm^2\ V^{-1}\ s^{-1}$ under ambient circumstances, stronger aggregation tendency, better crystallinity, lower LUMO level and UV and visible light stability are the most important properties which are observed in the synthesized polymers. Poly(p-phenylene vinylene)s (PPVs), or variants of PPVs, are among the most extensively studied *p*-type polymers in organic electronics. PPVs typically have electron mobilities below $10^{-4}\ cm^2\ V^{-1}\ s^{-1}$, which limits their use in organic photovoltaics and high-performance polymer FETs.

Ting *et al.*[48] synthesized new PPV derivative called benzodifurandione-based PPV (BDPPV), which is electron-deficient. This new PPV derivative overcomes common PPV flaws like conformational disorder, weak interchain interaction and high LUMO level to display high electron mobilities up to 1.1 $cm^2\ V^{-1}\ s^{-1}$ under ambient conditions (4 orders of magnitude higher than those of other PPVs). The first polymer capable of transporting electrons over 1 $cm^2\ V^{-1}\ s^{-1}$ in ambient circumstances is BDPPV.

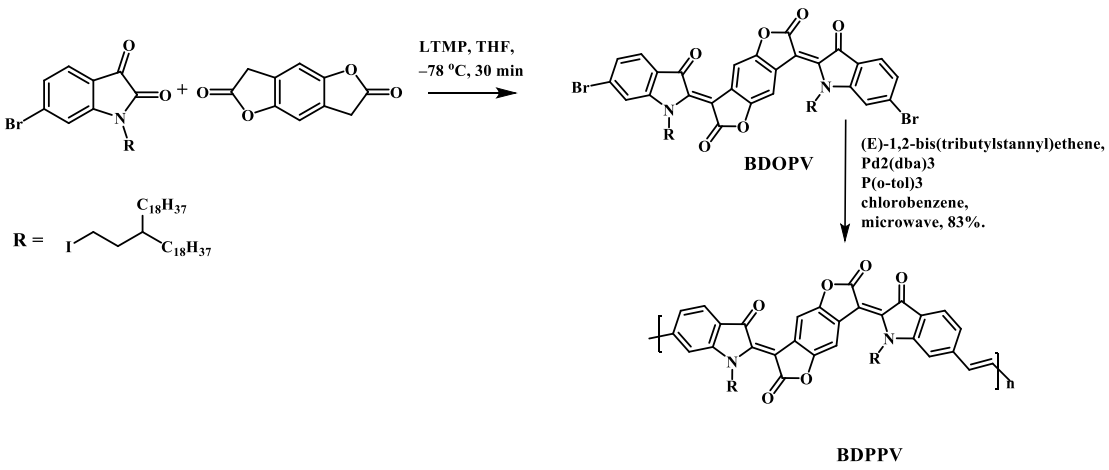

Figure 2.1 Synthesis of isoindigo-based polymer BDPPV.[48]

The electron-accepting building block called indeno[1,2-*b*]fluorene-6,12-dione (INDF) and two D-A conjugated polymers called PINDFTT and PINDFBT were synthesised by Deng *et al.*[49] Due to the lower electron-accepting characteristic of INDF, the INDF-based polymers showed high band-gaps, higher HOMO, and LUMO energy levels. With the maximum hole and electron mobilities of 0.51 cm^2 V^{-1} s^{-1} and 0.50 cm^2 V^{-1} s^{-1}, respectively, the INDF-polymers displayed highly balanced ambipolar properties. It showed that INDF is an extremely attractive building block as an electron acceptor in polymer semiconductors used in ambipolar OTFTs and other printed electronics.

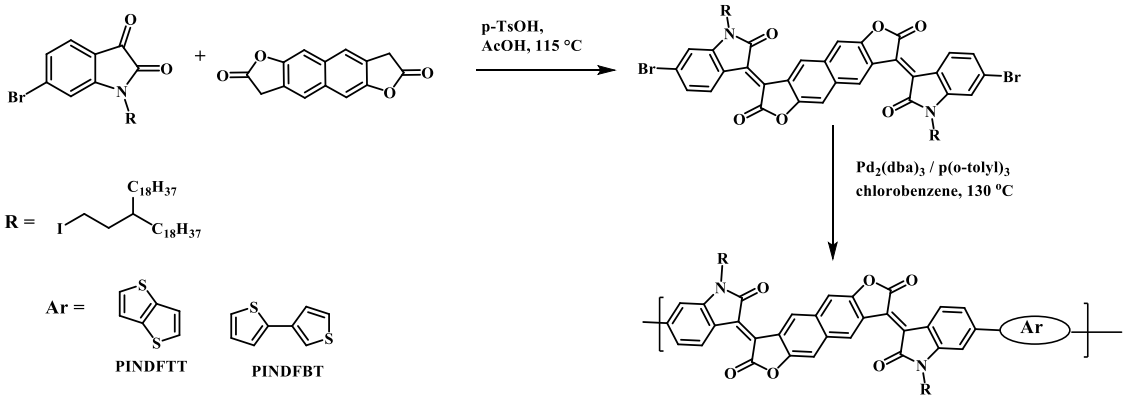

Figure 2.2 Synthesis of INDF-based monomer and polymers[49]

Ting *et al.*[50] have created two donor-acceptor copolymers, IIDDT and IIDT, in which the polythiophene backbone contains an isoindigo core. IIDDT showed the best field-effect performances, with a high mobility up to 0.79 cm^2 V^1 s^1 and an on/off ratio of 107. Due to their low-lying HOMO levels, it is noteworthy that these devices exhibit

excellent stability under ambient and high-humidity conditions. Additionally, these polymers are soluble in a common solvent, which is essential requirement for their device fabrication. Isoindigo-based polymers have great promise for use as solution-processable organic semiconductors for optoelectronic devices due to their ease of production and high mobility.

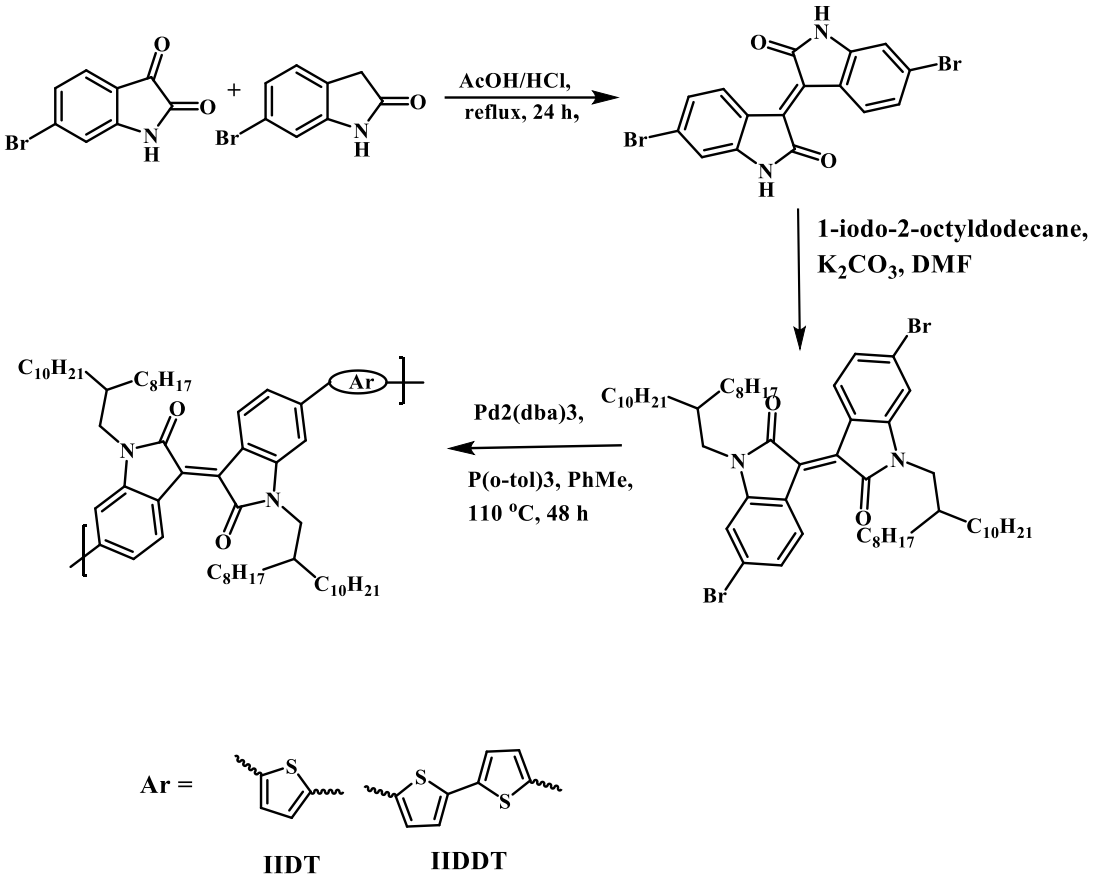

Figure 2.3 Synthesis of isoindigo-based polymers[50]

Long *et al.*[51] reported pyrazine-fused isoindigo-based conjugated polymers. The addition of a pyrazine ring in the middle of isoindigo results in high molar extinction coefficient and intramolecular hydrogen bonding. The Pyrazine-fused isoindigo (PzIIG) was created as an electron withdrawing unit, and two D-A conjugated polymer, PzIIG-BDT_2TC_8 and PzIIG-BTT_2TC_{10}, were created. Devices based on PzIIG-BDT_2TC_8 and PzIIG-BTT_2TC_{10} for inverted polymer solar cells showed Photo-Conversion Efficiencies (PCEs) of 5.26% and 3.36%, respectively. The Polymer Solar Cells (PSCs) built using PzIIG-BDT2TC8 showed high V_{oc} above 1.0 V. Optimising the device preparation conditions by increasing the morphology of active layers using

solvent vapour annealing (SVA) procedures and the choice of additives may result in further improvements to PSC performance.

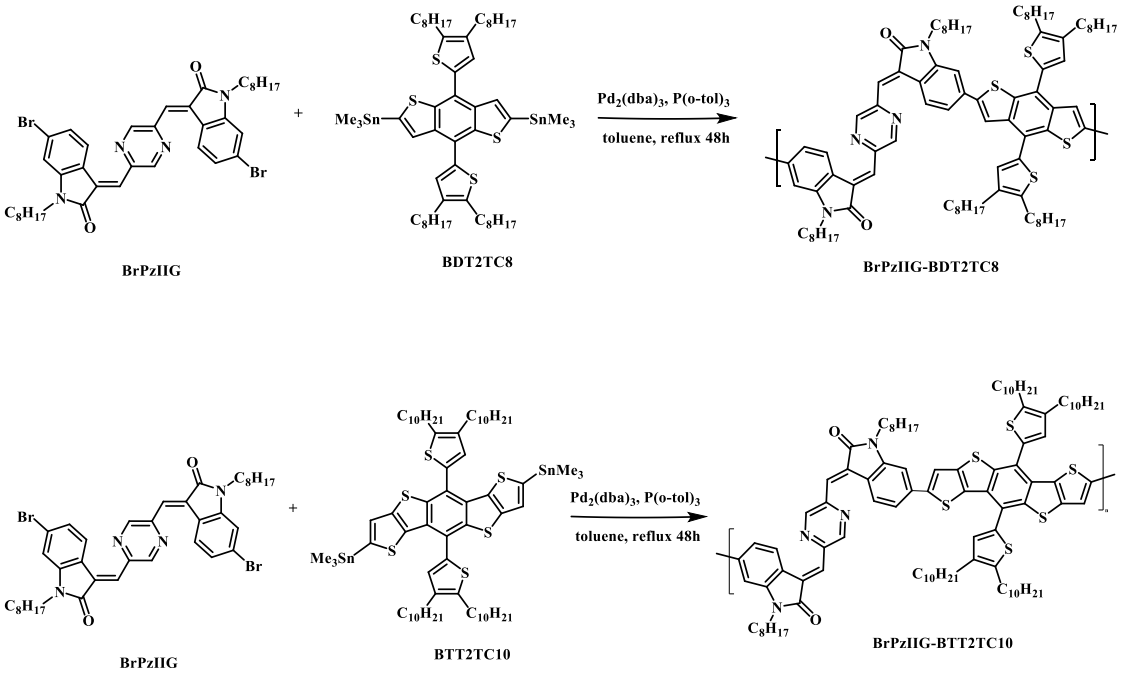

Figure 2.4 Synthesis of polymers, PzIIG-BDT2TC8 and PzIIG-BTT2TC10.[51]

Zhang *et* al.[52] reported two vinylidenedithiophenmethyleneoxindole (VDTOI). Due to the presence of S-O conformational locking, the centrosymmetric VDTOI unit has a unique acceptor-donor-acceptor structure and a very planar conjugated backbone. The VDTOI unit has characteristics structure having thiophene-flanked diketopyrrolopyrrole building block having the highest occupied molecular orbital (HOMO) and lowest unoccupied molecular orbital (LUMO), energy levels values of 5.35 eV and 3.42 eV, respectively. The structural characteristics suggest that VDTOI might be a promising component for creating polymeric semiconductors. The synthesized VDTOI-based copolymers, **P1** and **P2**, shows broad absorption spectra in the range of 330 nm to 740 nm and exhibit good heat stability. Their HOMO energy levels, which are around 5.40 eV, are in good agreement with the work function of a gold (Au) electrode (5.13 eV), which suggests that the Au electrodes effectively injected holes into the polymer semiconductor films. Field-effect transistors based on polymers, **P1** and **P2** demonstrated normal *p*-type transport properties. The device based on polymer **P1** shows the maximum mobility of 0.35 $cm^2 V^1 s^1$.

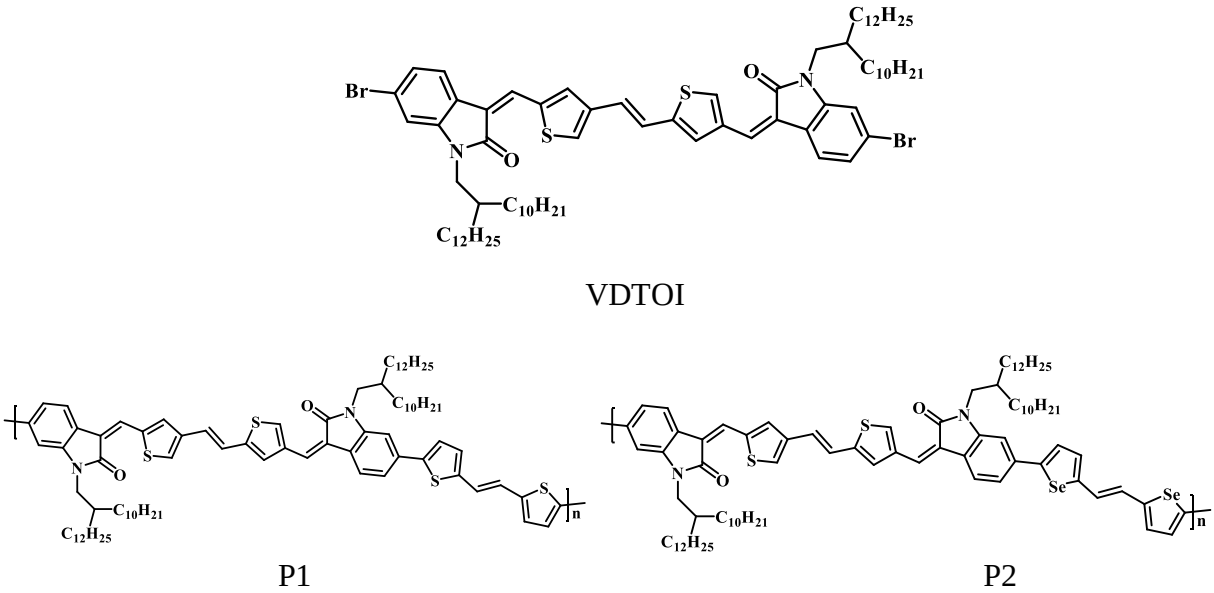

Figure 2.5 The chemical structures of VDTOI-based copolymers reported by Zhang *et al.*[52]

In the present work we have synthesized three π-extended, benzene-, dialkoxybenzene- and thiophene-fused isoindigo molecules. The D-A type conjugated polymers were synthesised by stille coupling reaction between 5,5'-bis(trimethylstannyl)-2,2'-bithiophene unit and π-extended isoindigo-based compounds using $Pd_2(dba)_3$ and tri-o-tolylphosphine as the catalyst-ligand system in refluxing toluene.

Results and discussion

Synthesis of monomers and polymers

The isoindigo-based monomers were synthesised by Knoevenagel-type condensation reaction between 5-bromo-*N*-tetradecylindolin-2-one and three different aldehydes using piperidene as base with different solvents under nitrogen atmosphere. The *n*-tetradecylindolin-2-one (compound **2**) is synthesized according to the reported literature process as per the Scheme 2.1.[53–55] 5-Bromoisatin is subjected to n-alkylation using potassium carbonate (K_2CO_3) and *n*-tetradecylbromide. The resulting compound **1** is subjected to Wolff-Kishner reaction using hydrazine hydrate.

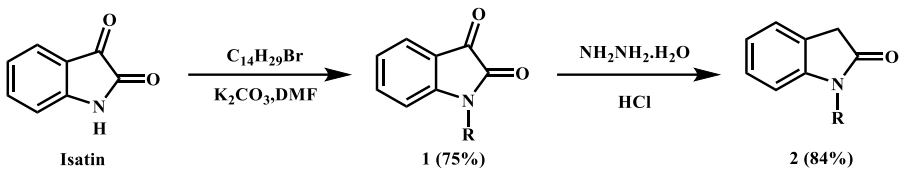

Scheme 2.1 Synthesis of 5-bromo-*N*-tetradecylindolin-2-one from 5-bromoisatin

Dialkoxy benzaldehyde (**7)** was synthesized from 1,4-dihydroxybenzene according to the literature procedure reported by Doddi *et al* [56] (Scheme 2.2). 1,4-Dihydroxy benzene was subjected to *n*-alkylation using potassium carbonate (K_2CO_3) and 1-bromododecane. The resulting product was reacted with paraformaldehyde and hydrobromic acid (HBr) to get compound **4**. Acetylation of compound **4** was carried out in presence of potassium acetate and tetra butyl ammonium bromide (TBAB) to get compound **5**. Reduction of compound **5** was carried out by using lithium aluminium hydride ($LiAlH_4$) and oxidation of the resulting product was carried out by pyridinium chlorochromate (PCC) to get the desired aldehyde **7**.

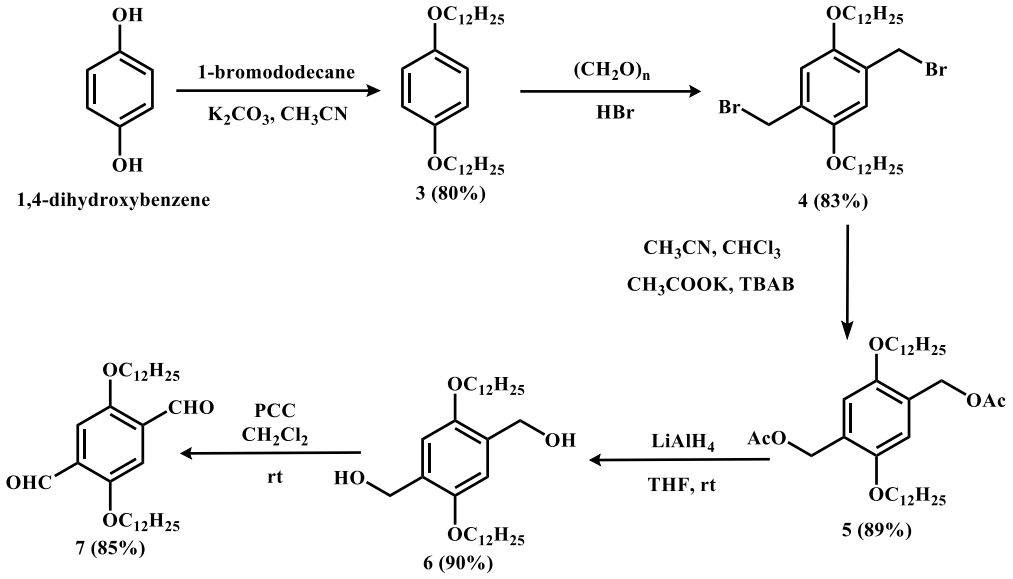

Scheme 2.2 Synthesis of compound **7** from 1,4-dihydroxybenzene

The π-extended benzene-, dialkoxybenzene-, and thiophene-fused isoindigo (compounds **TIIG**, **DAB**, and **THP**) are synthesized by Knoevenagel-type coupling reaction[57] between *n*-tetradecylindolin-2-one (compound **2**) and corresponding dialdehydes (terephthalaldehyde, compound **7**, and thiophene-2,5-dicarbaldehyde) using piperidine as base as per Scheme 2.3

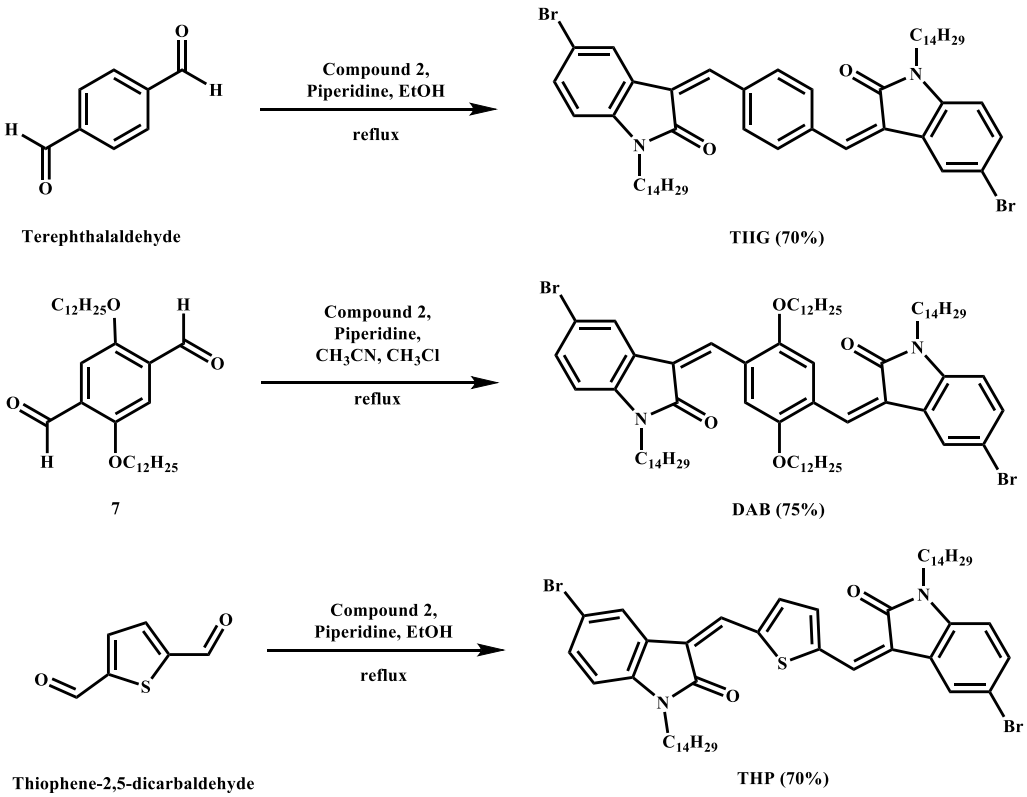

Scheme 2.3 Synthesis of π-extended isoindigo compounds, **TIIG**, **DAB**, and **THP.**

The π-extended isoindigo based D-A type conjugated polymers namely **TIIG-P**, **DAB-P** and **THP-P** were synthesised by stille coupling reaction between 5,5'-bis(trimethylstannyl)-2,2'-bithiophene unit and π-extended isoindigo compounds **TIIG**, **DAB** and **THP** using $Pd_2(dba)_3$ and tri-o-tolylphosphine as the catalyst-ligand system in refluxing toluene (Scheme 2.4). The obtained crude polymers **TIIG-P**, **DAB-P** and **THP-P** are purified by sequential soxhlet extraction technique using methanol, petroleum ether, toluene and chloroform, respectively. The solvent was evaporated under reduced pressure and polymers were collected and dried under vacuum at 60 ℃.

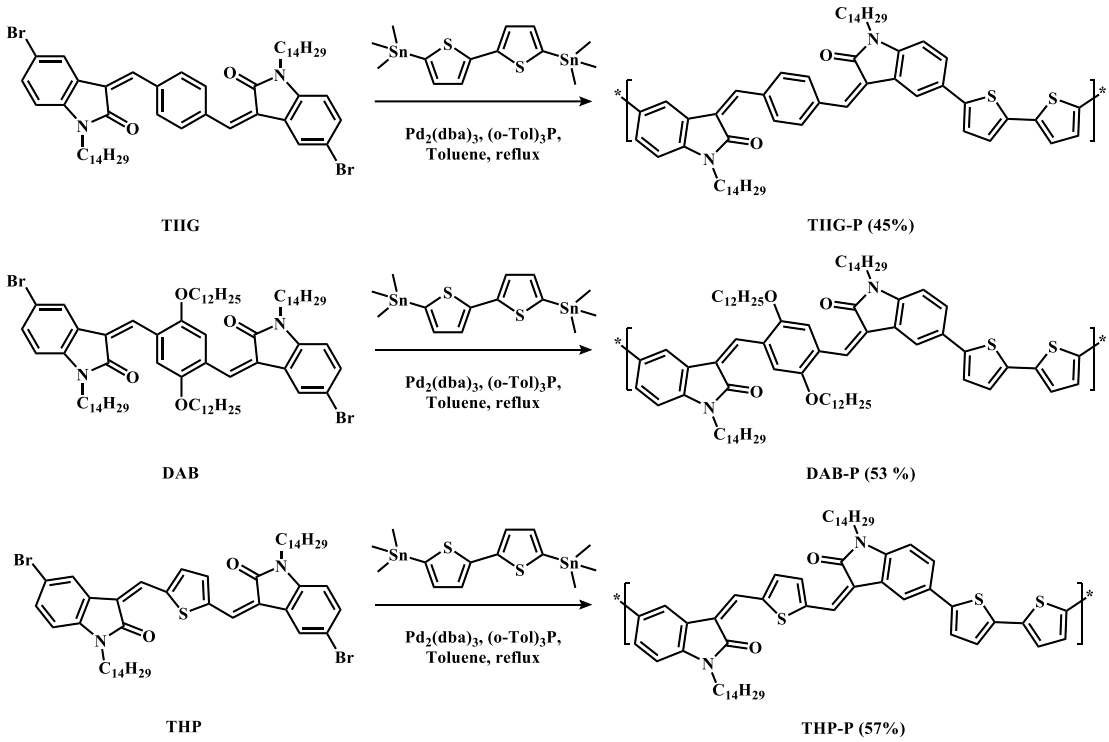

Scheme 2.4 Synthesis of π-extended D-A-type conjugated polymers.

Molecular weight and thermal properties of polymers

The π-extended isoindigo-based conjugated polymers, **TIIG-P**, **DAB-P** and **THP-P** were synthesized by stille coupling reaction showed weight average molecular weights (M_W) in the range of 10 kDa to 12 kDa. Incorporation of alkyl chain in the monomers increase the solubility of the resulting polymers. All the synthesized polymers showed moderate to good solubility properties in the common organic solvents like dichloromethane, chloroform and tetrahydrofuran. Thermal properties of all synthesized conjugated polymers were analyzed by thermogravimetric analysis (TGA) at a heating rate of 10 ℃/min under nitrogen atmosphere (Figure 2.6). The decomposition temperature (T_d) of all polymers were defined as the temperature at

which the polymer losses its weight by 5%. All the synthesized polymers show decomposition temperature above 200 ℃, which shows their sufficiently high thermal stability for application in any organic solar cells. Weight average molecular weight (M_W), poly dispersity index (PDI) and decomposition temperature (T_d) of the π-extended isoindigo-based conjugated polymers are summarised in table 2.1.

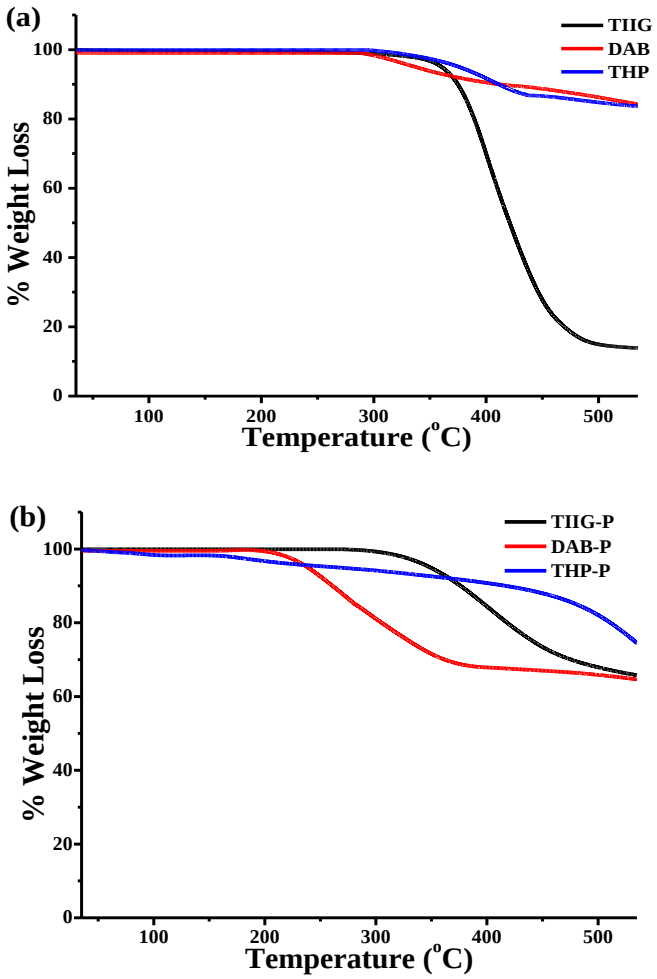

Figure 2.6 Thermogravimetric analysis (TGA) of (a) π-extended isoindigo compounds **TIIG, DAB** and **THP**; and (b) π-extended D-A-type conjugated polymers **TIIG-P** (black line), **DAB-P** (red line) and **THP-P** (blue line).

Photophysical properties of monomers

The photophysical properties of π-extended isoindigo-based conjugated monomers and polymers were studied by UV-visible spectroscopy in a dilute chloroform solution of polymer. The isoindigo-based polymers show single absorption spectrum in chloroform solution. As shown in Figure 2.7. **TIIG** and **DAB** exhibit relatively broader absorption bands corresponding to the π-π* transitions with absorption maxima (λ_{max}) at 392 nm and 379 nm, respectively and extending near to 430 nm. **THP** showed absorption maxima (λ_{max}) at 451 nm, which is much bathochromically shifted compared to compounds **TIIG** and **DAB**.

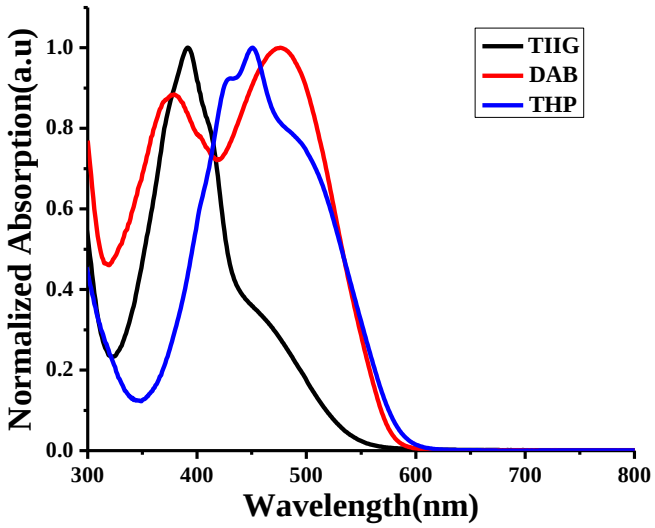

Figure 2.7 UV-vis spectra of monomers.

Planarization of the molecule and the orientation of the central unit with respect to the terminal indolinone units both play important roles in increasing the conjugation length. Intense charge transfer bands in the UV-visible absorption spectra are also indicative of the planarity and extended conjugation within the conjugated molecules.[58] The less intense transition band between 340 – 440 nm in the absorption spectrum of **TIIG** can be related to the planar structure of **TIIG**. The transition band in **DAB** appears red-shifted and is moderately intense, having absorption maximum (λ_{max}) at 476 nm, whereas that of **THP** appears as the most intense and red-shifted shoulder peak at 474 nm, which is extended up to 580 nm. The most intense band for **THP** can be related to the better coplanarity and extended π-conjugation of the molecule resulting from non-bonding interactions between the sulphur atom of the central thiophene unit and carbonyl oxygen atom of the terminal indolinone units.[37]

Photo physical properties of polymers

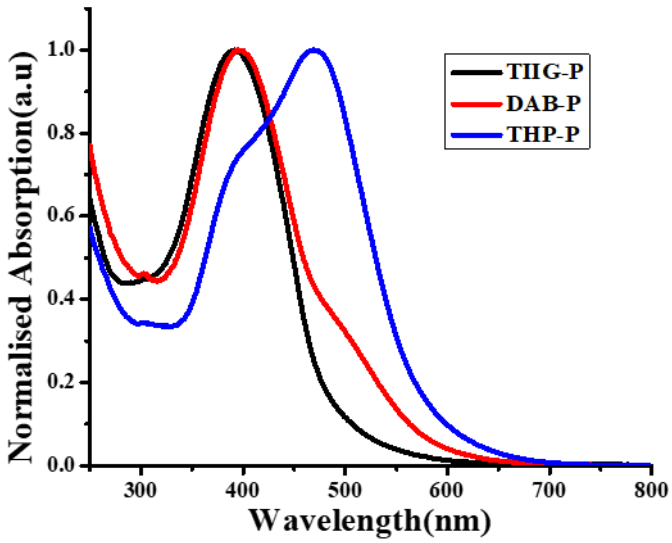

Figure 2.8 UV-vis spectra of polymers.

Polymer **TIIG-P** exhibits π-π* transition band with absorption maximum (λ_{max}) at 486 nm, while polymer **DAB-P** shows π-π* transition band with absorption maximum (λ_{max}) at 575 nm (Figure 2.8). The π-π* transition band of polymer **THP-P** has absorption maximum (λ_{max}) at 576 nm with shoulder peak at 391 nm. The optical band-gaps (E_g^{opt}) of the polymers, **TIIG-P**, **DAB-P** and **THP-P** are found to be 2.55 eV, 2.16 eV and 2.15 eV, respectively. The photophysical properties of the synthesized polymers are summarized in Table 2.1.

Table 2.1 Photophysical properties of π-extended isoindigo compounds **TIIG, DAB** and **THP** and their conjugated polymers **TIIG-P**, **DAB-P** and **THP-P**

Compound	λ_{max} (nm)	λ_{edge} (nm)	E_g^{opt} (eV)[a]	T_d (°C)	M_w (Dalton)	PDI (Đ)
TIIG	392	532	2.33	360	--	--
DAB	379, 476	577	2.15	337	--	--
THP	451	583	2.12	376	--	--
TIIG-P	393	486	2.55	349	12054	1.39
DAB-P	398	575	2.16	238	12827	1.72
THP-P	470	573	2.15	265	19091	1.61

Decomposition temperature T_d (obtained from TGA), Molecular weight M_w and poly-dispersity index (Đ, obtained from GPC analysis) of conjugated polymers **TIIG-P**, **DAB-P** and **THP-P**; [a] calculated using equation $E_g^{opt} = 1240/\lambda_{edge}$.

Electrochemical properties of monomers

The frontier orbital energy level of the synthesised three novel iso-indigo-based monomers were measured by cyclic voltammetry (CV). CV experiments are carried out in the dry acetonitrile-chloroform (7:3) solution using tetra-*n*-butylammonium hexafluorophosphate ($TBAPF_6$) as a supporting electrolyte (~50 mM). Three electrode system comprised of a Pt disc electrode as the working electrode, a Pt wire electrode as the counter electrode and Ag/Ag^+ as the reference electrode were used. Compounds, **TIIG**, **DAB** and **THP** are dissolved in dry acetonitrile-chloroform (7:3) solution (~5 mM), degassed with nitrogen gas and subjected to the CV measurements.

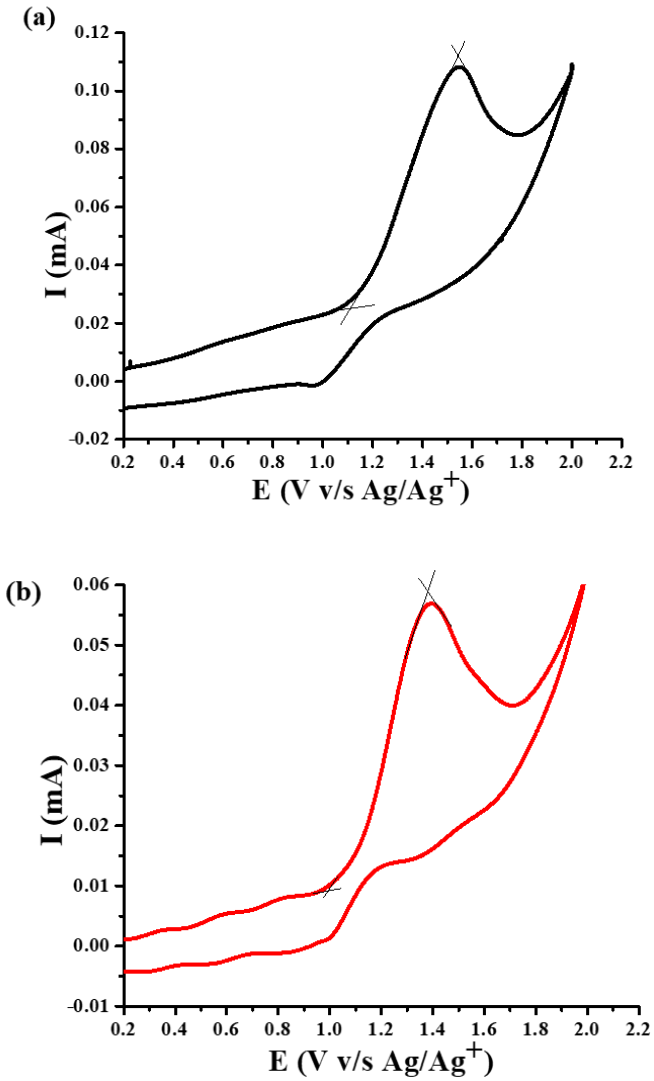

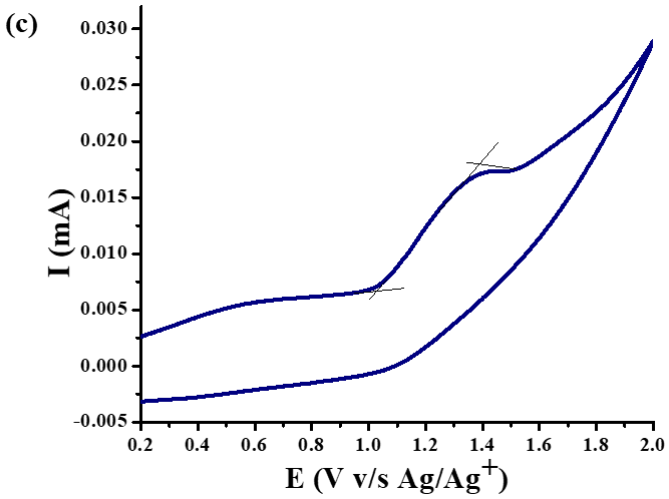

Figure 2.9 Oxidation curves of compounds (a) **TIIG** (b) **DAB** and (c) **THP**, obtained by cyclic voltammetry at 50 mV/s in dry acetonitrile-chloroform (7:3) using $TBAPF_6$ as a supporting electrolyte; $\boldsymbol{E_{onset\ Fc/Fc^+} = 0.50\ V}$.

All three monomers showed irreversible oxidation waves in the cyclic voltammogram (Figure 2.9). The oxidation potentials of monomers, **TIIG**, **DAB** and **THP** were measured from the oxidation waves and they are found to be at +1.54 V, +1.39 V, and +1.40 V, with onset oxidation potentials of +1.15 V, +1.07 V, and +1.02 V, respectively. The corresponding HOMO energy levels are calculated from the onset oxidation potentials. The HOMO energy levels of compounds, **TIIG**, **DAB** and **THP** were found to be at −5.45 eV, −5.37 eV and −5.32 eV, respectively. The LUMO energy levels are calculated using the equation: $E_{LUMO} = E_{HOMO} + E_g^{opt}$ and are found to be at −3.12 eV, −3.22 eV and −3.20 eV, respectively for compounds, **TIIG, DAB** and **THP**. The electrochemical properties of synthesised iso-indigo based monomers are summarized in table 2.2.

Electrochemical properties of polymers

The frontier orbital energy levels of the synthesised π-extended iso-indigo based conjugated polymers were measured by using cyclic volyammetry (CV). CV experiments are carried out in the dry acetonitrile-chloroform (7:3) solution using tetra-*n*-butylammonium hexafluorophospate ($TBAPF_6$) as a supporting electrolyte (~50 mM) using a three-electrode system: a Pt disc electrode as the working electrode, a Pt wire electrode as the counter electrode and Ag/Ag^+ as the reference electrode. Compounds,

TIIG-P, **DAB-P** and **THP-P** are dissolved in dry acetonitrile-chloroform (7:3) solution (~5 mM), degassed with nitrogen gas and subjected to the CV measurements.

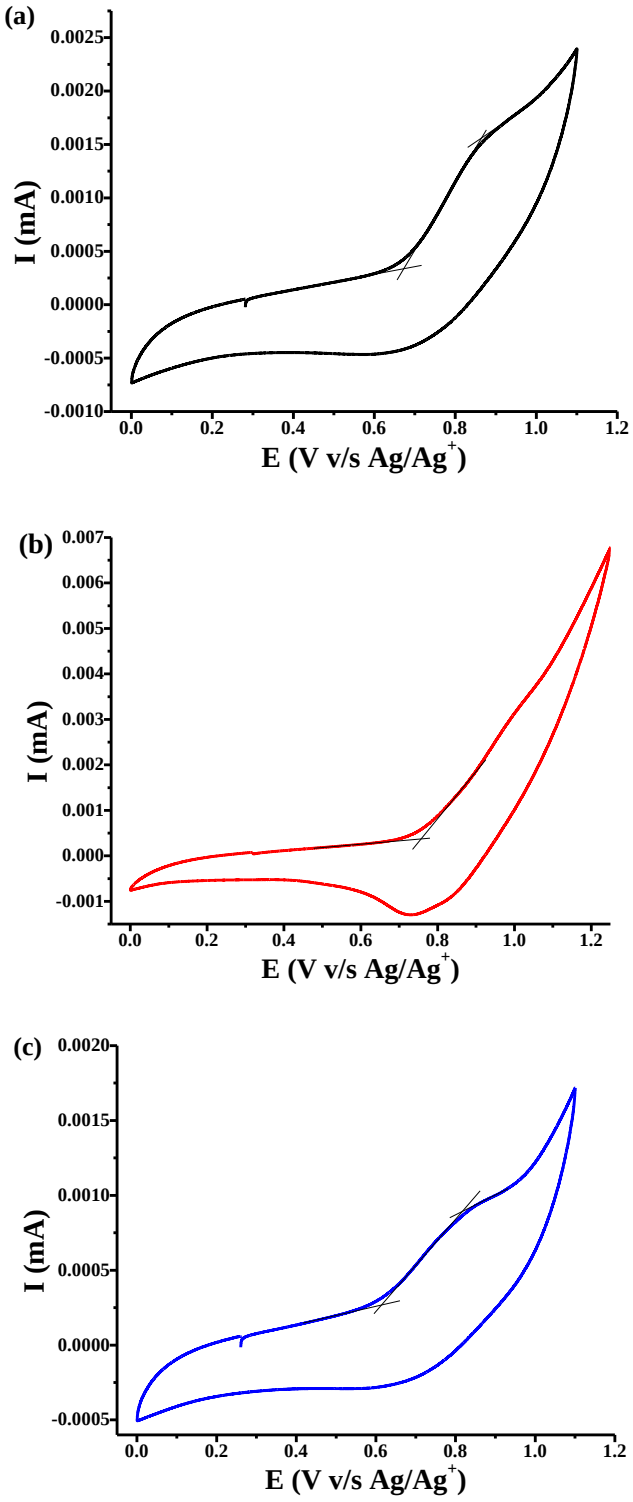

Figure 2.10 Oxidation curves of compounds, (a) **TIIG-P** (b) **DAB-P** and (c) **THP-P** obtained by cyclic voltammetry at 50 mV/s in dry acetonitrile-chloroform (7:3) using $TBAPF_6$ as a supporting electrolyte; $\boldsymbol{E_{onset\ Fc/Fc^+} = 0.50\ V}$.

All the three synthesized polymers show irreversible oxidation potential waves in cyclic voltammogram (Figure 2.10). The oxidation potential of **TIIG-P** and **THP-P** were measured from oxidation waves and they are found to be at +0.87 V and +0.82 V, whereas the oxidation potential of polymer **DAB-P** results in an unresolved oxidation peak. The onset oxidation potentials were found to be at +0.67 V, +0.76 V, and +0.61 V for polymers, **TIIG-P**, **DAB-P,** and **THP-P,** respectively. (Figure 2.9 a, b, and c). The corresponding HOMO energy levels are calculated from the onset oxidation potentials and found to be at −4.97 eV, −5.06 eV, and −4.91 eV, respectively. Electrochemical studies revealed that the central thiophene unit containing π-extended isoindigo-based conjugated polymer **THP-P** exhibit elevated HOMO energy levels compared to the **TIIG-P** and **DAB-P** due to the electron-donating nature of the thiophene unit. The LUMO energy levels are calculated using the equation: $E_{LUMO} = E_{HOMO} + E_g^{opt}$ and are found to be at −2.42 eV, −2.90 eV and −2.76 eV, respectively, for polymers **TIIG-P**, **DAB-P,** and **THP-P**. The electrochemical properties of the polymers are summarized in Table 2.2.

Table 2.2 Electrochemical properties of π-extended isoindigo-based compounds, **TIIG, DAB** and **THP** and their conjugated polymers, **TIIG-P**, **DAB-P** and **THP-P**

Compound	E_{oxi} (V) [a]	$E_{oxi,onset}$ (V) [a]	E_{HOMO} (eV) [b]	E_{LUMO} (eV) [c]
TIIG	+1.54	+1.15	−5.45	−3.12
DAB	+1.39	+1.07	−5.37	−3.22
THP	+1.40	+1.02	−5.32	−3.20
TIIG-P	+0.87	+0.67	−4.97	−2.42
DAB-P	-[d]	+0.76	−5.06	−2.90
THP-P	+0.82	+0.61	−4.91	−2.76

[a]potential v/s Ag/Ag^+; [b]calculated from equation $\boldsymbol{E_{HOMO} = -(E_{onset\ oxi} + 4.8 - E_{onset\ Fc/Fc^+})}$; [c]calculated from equation $\boldsymbol{E_{LUMO} = E_{HOMO} + E_g^{opt}}$; [d] unresolved peak.

Computational studies

Density functional theory (DFT) is a computational quantum mechanical method used to study the electronic structure of molecules and materials. Theoretical calculations for three different monomers **TIIG, DAB** and **THP** as well as their corresponding polymers **TIIG-P**, **DAB-P**, and **THP-P** was carried out by using the B3LYP/6-31G(d) basic set on model compounds (by replacing N-alkyl by N-ethyl groups).[59,60] The theoretically calculated HOMO-LUMO gap values are found to be 2.91 eV, 3.06 eV and 2.51 eV for monomers **TIIG**, **DAB** and **THP** replacing N-alkyl by N-ethyl groups). The theoretically calculated HOMO-LUMO gap values are found to be 2.91 eV, 3.06 eV and 2.51 eV for monomers **TIIG, DAB** and **THP** respectively (Table 2.3). **THP** showed lowest HOMO-LUMO gap, which indicates that thiophene containing system is more conjugated than the other two monomers, **TIIG** and **DAB**.

Table 2.3 DFT (B3LYP/6-31G(d)) calculated structures, HOMO and LUMO of monomers, **TIIG, DAB** and **THP,** respectively.

Compound	HOMO	LUMO	Band gap (eV) ΔE=(LUMO-HOMO)
TIIG	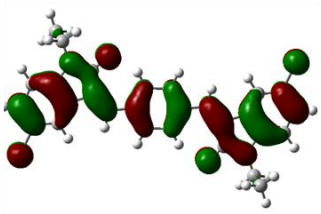	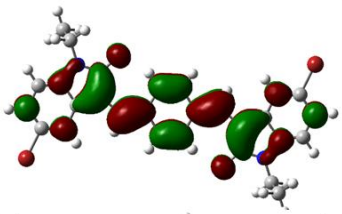	2.91eV
DAB	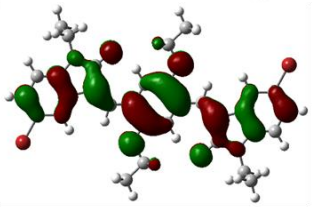	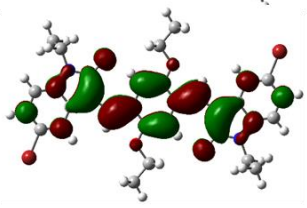	3.06 eV
THP	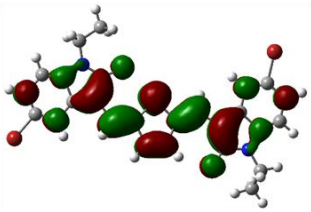	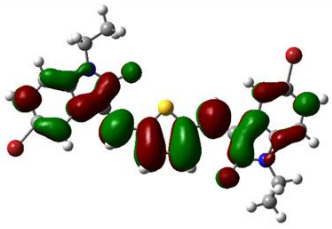	2.51 eV

At the B3LYP/6-31G(d) level, model polymers, **TIIG-P**, **DAB-P**, and **THP-P** were optimized. According to the optimized polymer structures, **TIIG-P** and **DAB-P** are linear polymers, but **THP-P** has a wavy arrangement of their comonomers (Figure

2.12). Model polymers, **TIIG-P**, **DAB-P** and **THP-P** are found to have band gap values of 2.21 eV, 2.21 eV and 2.11 eV, respectively. The HOMO and LUMO of the all polymers are displayed in Figure 2.11 which clearly shows LUMO are concentrated on the π-extended isoindigo portions and HOMO are delocalized over the entire molecule.

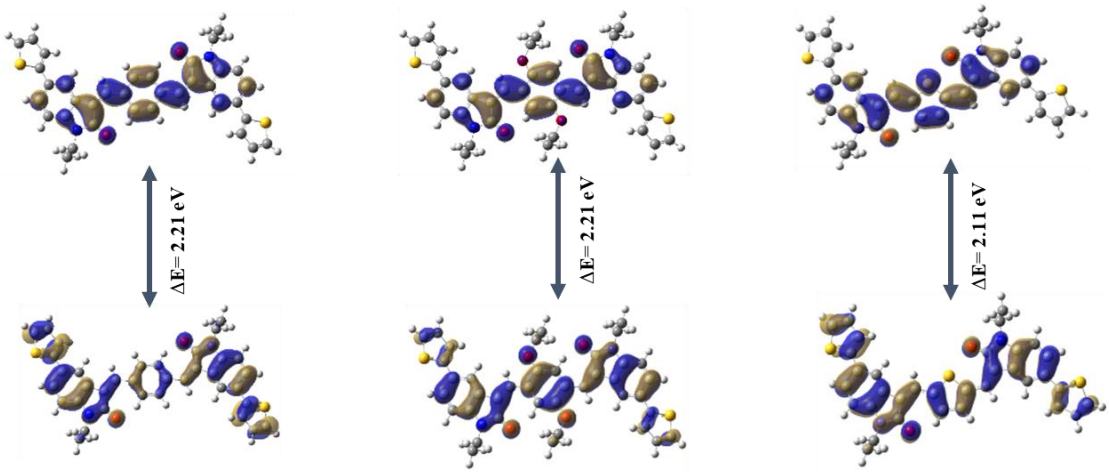

Figure 2.11 DFT (B3LYP/6-31G(d)) calculated structures, HOMO and LUMO of model polymers, **TIIG-P, DAB-P** and **THP-P**, respectively.

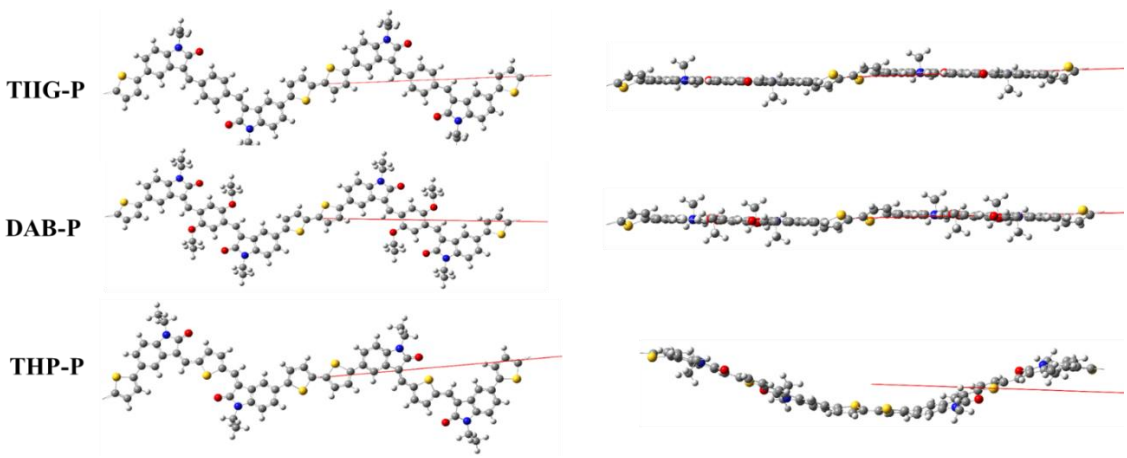

Figure 2.12 Optimized structures of polymers **TIIG-P, DAB-P** and **THP-P** at B3LYP/6-31G(d) level (red lines indicate the propagation vectors).

X-ray diffraction studies of polymers

The powder X-ray diffraction (PXRD) analysis depicted in Figure 2.13 reveals notable insights into the structural characteristics of polymer films, **TIIG-P, DAB-P** and **THP-P**. A distinctive broad peak, observed at approximately 2θ = 20.67°, underscores the inherent amorphous nature of these polymers. Remarkably, a shared π-π stacking distance of 4.29 Å among the polymers suggesting a consistent structural feature.

Moreover, a nuanced examination of the diffraction peaks suggests a progressive increase in crystalline behaviour, with polymer **THP-P** exhibiting greater crystallinity compared to polymer **TIIG-P** and polymer **TIIG-P** surpassing polymer **DAB-P** in this aspect. This observation adds depth to our understanding of the polymers structural arrangement, with implications for their material properties and potential applications.[61]

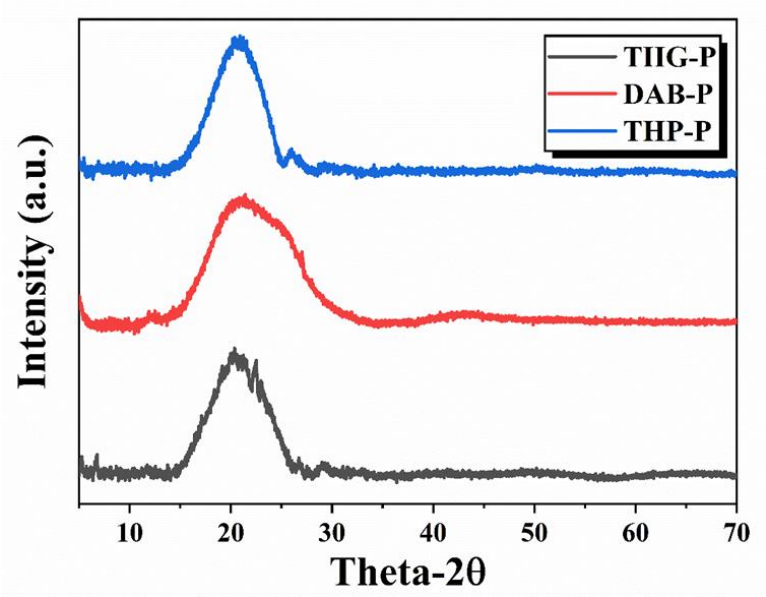

Figure 2.13 Powder X-ray diffraction pattern spectra of polymers, **TIIG-P, DAB-P** and **THP-P**.

Space Charge Limited Current (SCLC) measurement of polymers

The assessment of the hole-transporting capabilities of the synthesized polymers are carried out by using the Space-Charge-Limiting Current (SCLC) technique. This was carried out through the utilization of a specialized hole-only device designed for precise measurement of the hole mobility of the polymers (Figure 2.14).

The hole-only device architecture comprises FTO/NiOx/Polymer/MoO_3/Al with an active area of 0.12 cm^2. The preparation of the FTO glass slides involved a thorough cleaning process, which included sonication in a soapy solution, followed by rinsing in deionized water, acetone, and isopropyl alcohol (IPA), each for a duration of 15 minutes. Subsequently, the FTO slides were dried and subjected to UV-ozone treatment. After that the spin coating of the NiO_x precursor solution, which was uniformly applied to the FTO glass surface at a speed of 3500 rpm for a duration of 45 seconds. Following this, the coated glass underwent annealing at 300 °C for 1 hour under ambient conditions, resulting in the formation of a hole transport layer (HTL) with a thickness of approximately 120 nm. The polymers dissolved in chloroform were spin-coated at 1000 rpm for 60 seconds, followed by annealing at 80 °C for 10 minutes. A thin layer of MoO_3, serving as a buffer layer, was thermally deposited to a thickness of 20 nm. Finally, a shadow mask was utilized to thermally deposit a 100 nm-thick Al metal electrode. Current density-voltage characteristics were measured using a CHI660E instrument (CHI Instrument, Inc., Austin, TX) at a scanning rate of 100 mV/s.

Hole motilities of polymers were calculated using the Mott– Gurney equation.[59,62,63]

$$J = \frac{9}{8}\varepsilon_0\varepsilon_r\mu\frac{V^2}{L^3}$$

where, J is the current density, μ is the hole mobility, ε_o is the vacuum permittivity (8.85 × 10^{-12} Fm^{-1}), ε_r is the dielectric constant of the material (considered as 3 for organic semiconductors), d is the film thickness, and V is the applied voltage.

(a)

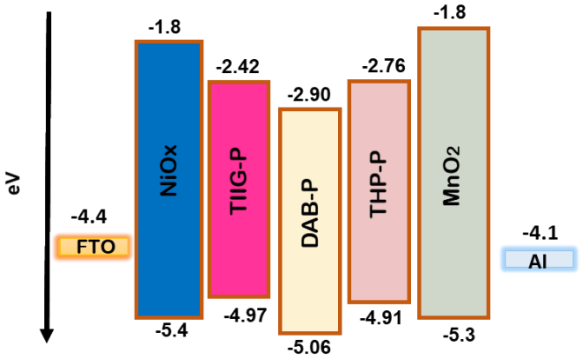

(b)

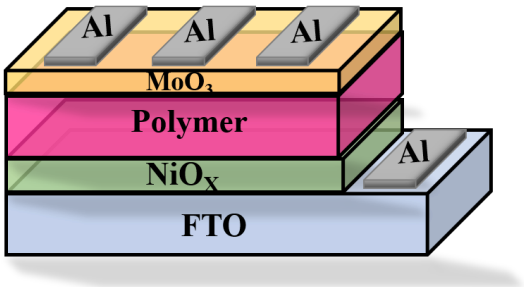

Figure 2.14 (a) The energy level diagram of polymers, **TIIG-P, DAB-P** and **THP-P** (b) Schematic diagram of a hole-only device.

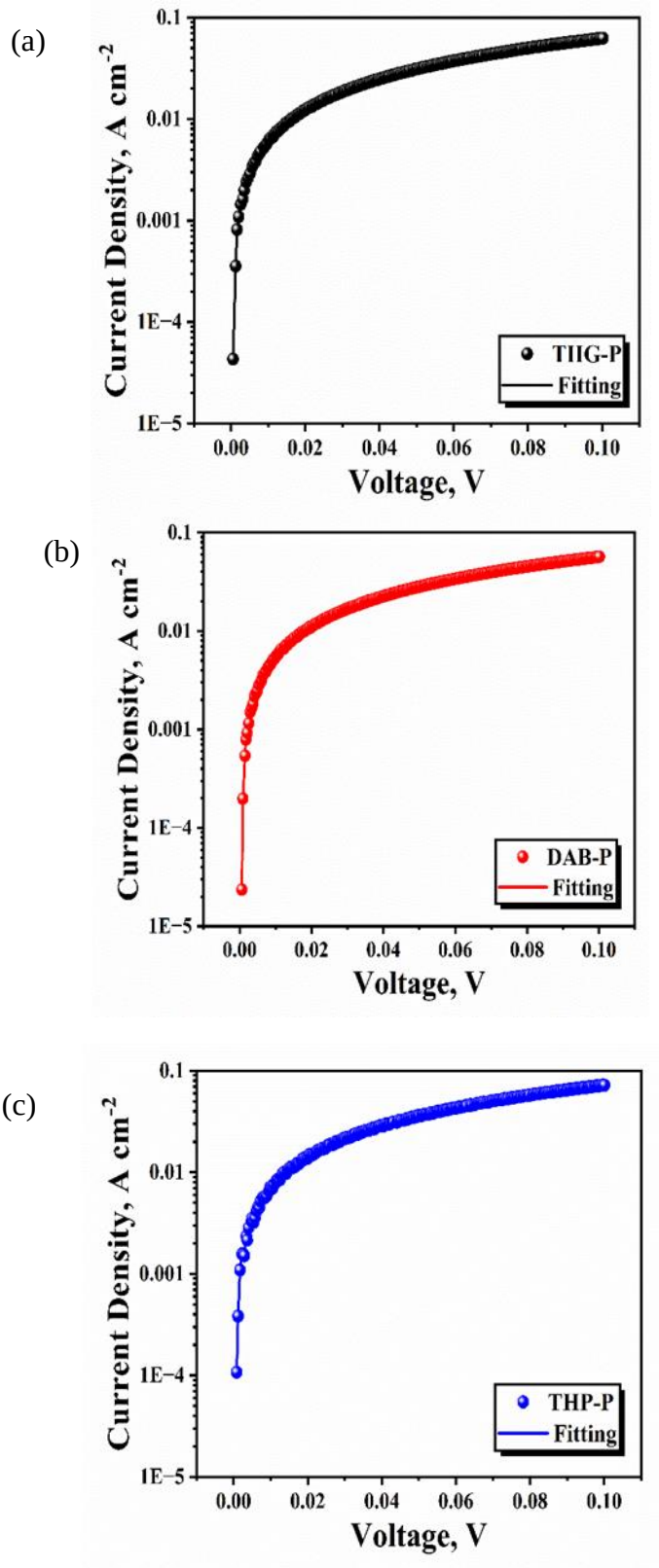

Figure 2.15 SCLC hole motilities of polymers, **TIIG-P, DAB-P** and **THP-P.**

The measured SCLC hole mobilities were found to be 7.11×10^{-2} cm^2 V^{-1} s^{-1}, 6.43×10^{-2} cm^2 V^{-1} s^{-1} and 8.19×10^{-2} cm^2 V^{-1} s^{-1} for polymers, **TIIG-P, DAB-P** and **THP-P**, respectively (Figure 2.15). The obtained values of hole mobilities were quite good and the devices of such polymers with high hole mobilities can showed potential photovoltaic properties.

Conclusion

Isoindigo-based D-A type conjugated molecules are synthesised by Knoevenagel coupling reaction. The polymerization of all three monomers are carried out by using 5,5'-bis(trimethylstannyl)-2,2'-bithiophene to form conjugated low band-gap D-π-A polymers. The synthesised iso-indigo based polymers showed moderate to good solubility in the common organic solvents. All three polymers have sufficiently high thermal stability. Polymers, **TIIG-P**, **DAB-P** and **THP-P** were characterised and studied photophysically and electrochemically. All the polymers showed good absorptivity in the visible and near IR region. Photophysical properties of polymers, **TIIG-P, DAB-P** and **THP-P** shows broad absorption spectra and the band gap values were found to be at 2.55 eV, 2.16 eV and 2.15 eV, respectively. Electrochemical studies of polymer revealed that all the polymers showed lower HOMO (below -4.9 eV) and LUMO (below -2.4 eV) energy levels and low electrochemical band gap compared to the synthesized monomers due to the extended delocalization of π-electrons. The structural aspects of polymers, **TIIG-P**, **DAB-P** and **THP-P** were studied by DFT calculations on model polymers (by replacing *N*-alkyl by *N*-ethyl groups) comprising of the repeat unit of each parent copolymer indicates that the polymers are highly planner with the dihedral angle less than 30°. The calculated band gap values for model polymers, **TIIG-P, DAB-P** and **THP-P** were found to be 2.11 eV, 2.21 eV and 2.11 eV, respectively. The preliminary characterization data showed that the new synthesized conjugated polymers, **TIIG-P**, **DAB-P** and **THP-P** were potential candidates for organic electronic devices.

Experimental procedures

General procedure

All the chemicals are reagent grade and are used as purchased. Moisture sensitive reactions are performed under inert atmosphere under dry nitrogen by using dry solvents. Reactions are monitored by thin-layer chromatography (TLC) using Merck 60 F254 aluminium-coated plates and the spots are visualized under ultraviolet (UV) light. Column chromatography is carried out on silica gel (60–120 mesh).

^{1}H and ^{13}C NMR spectra are recorded on a Bruker Avance-III 400 spectrometer in $CDCl_3$ and DMSO-D6. The high resolution mass spectra are recorded on Xevo G2-XS QTOF Mass Spectrometer. Thermogravimetric analysis (TGA) is done on Exstar SII TG/DTA 6300 using N_2 as an inert gas. Molecular weights of the polymer samples are measured with Agilent 1260 Infinity GPC instrument, equipped with RI detector. Polystyrene is used as a calibration standard. Polymer sample (~5 mg) are dissolved in THF (~5 mL) and are filtered through a 0.2 µ filter. The analysis is done using THF as an eluent at a flow rate of 1-2 mL/min. UV-Visible absorption spectra are recorded on Jasco FP 6300 spectrofluorometer using quartz cuvette. Electrochemical studies are carried out by using an Electro Chemical Analyser, Model SP-200, Biologics Sas France Make using a platinum (Pt) disk electrode as a working electrode, a platinum wire as a counter electrode and a AgCl-coated Ag wire as a reference electrode. Non-aqueous Ag/Ag^{+} wire is prepared by dipping silver wire in a solution of $FeCl_3$ and HCl. Pt-disk electrodes were polished with alumina and washed with water and acetone and were dried with nitrogen gas before use to remove any incipient oxygen. All electrochemical potentials are reported against Ag/Ag^{+} taking ferrocene as an external standard; $E_{(onset(Fc/Fc)+)} = 0.50$ V

Synthesis of 5-bromo-1-tetradecylindolin-2-one

Compound **1** was synthesized according to the modified literature procedure reported by Li et al[53,64] while compound **2** was synthesized according to the modified literature procedure reported by Bura et al[65].

Synthesis of 5-bromo-1-tetradecylindoline-2,3-dione (1): 5-Bromoisatin (2g ,8.84 mmol) and potassium carbonate (K_2CO_3) (5.48g, 39.7 mmol) was added to 20 mL anhydrous DMF under nitrogen atmosphere and reaction mixture was stir at 60 ℃ for

10-15 min. To this stirred solution tetradecyl bromide (4.2 g, 15.47 mmol) was added in a dropwise manner. After that reaction mixture was allowed to stir at 80 ℃ for 3h, after cooling to room temperature reaction mixture was poured in to water and extracted with ethyl acetate. The combined organic layer was washed with water and dried over Na_2SO_4 and solvent was evaporated under reduced pressure. The crude product was purified by column chromatography over silica gel and pure product was eluted using 10% ethyl acetate-petroleum ether mobile phase.

5-Bromo-1-tetradecylindoline-2,3-dione (1): Dark orange solid. (1.83g, 49%); ^{1}H NMR (400 MHz, $CDCl_3$): δ 7.67 (d, J3 = 1.2 Hz, 1H), 6.79 (d, J2 = 7.6 Hz, 1H), 6.82 (dd, J2 = 7.6 Hz, J3 = 1.2 Hz, 1H), 3.70−3.74 (t, J2 = 7.2 Hz, 2H), 1.65−1.73 (m, 2H), 1.29−1.34 (m, 18H), 0.85−0.89 (t, J2 = 7.2 Hz, 3H).

Synthesis of 5-bromo-1-tetradecylindolin-2-one (2): Compound **1** (1.5g, 3.55mmol) and hydrazine hydrate 99% (8.88g, 177.5mmol) was taken in a two necked round bottom flask and refluxed at 140 ℃ for 1 h. After cooling to room temperature, the reaction mixture was poured in to water and extracted with ethyl acetate, washed with water and dried over anhydrous sodium sulphate the solvent was evaporated under reduced pressure. To the resulting crude, 20 mL of 6N aqueous hydrochloric acid is added and resulting mixture was heated at 60 ℃for 3h. The reaction mixture was poured in to 200 mL of water and extracted with ethyl acetate. Combined organic layer was washed with water, brine, dried over anhydrous sodium sulphate and evaporated under reduced pressure. The crude product was purified by column chromatography over silica gel and pure product was eluted using 40% ethyl acetate-petroleum ether as mobile phase.

5-Bromo-1-tetradecylindolin-2-one (2): Pale yellow solid. (1.24g, 84%); ^{1}H NMR (400 MHz, $CDCl_3$): δ 7.39 (d, J2 = 8.0 Hz, 1H), 7.26 (s, 1H), 6.768 (d, J2 = 8.0 Hz, 1H), 3.65−3.68 (t, J2 = 7.6 Hz, 2H), 3.51 (s, 2H), 1.62−1.66 (m, 2H), 1.25−1.32 (m, 18H), 0.86−0.90 (t, J2 = 7.2 Hz, 3H).

Synthesis of 2,5-bis(hydroxymethyl)benzene-1,4-dialdehyde

Synthesis of 1,4-bis(dodecyloxy)benzene (3): 1,4-Hydroxybenzene (5g ,45mmol) and potassium hydroxide (KOH) (7.63g ,136mmol) was added to 50 mL acetonitrile under nitrogen atmosphere and the reaction mixture was stirred at room temperature for 10 minutes. To this stirred solution dodecyl bromide (32.4g, 135mmol) was added and the

reaction mixture was refluxed for 12h. After completion of reaction, the reaction mixture was poured in to 200 mL of water and extracted with ethyl acetate. The combined organic phase was washed with water, dried over anhydrous sodium sulphate and concentrated under reduced pressure. The crude product was purified by column chromatography over silica gel and the pure product was eluted using 10% ethyl acetate-petroleum ether as mobile phase.

1,4-Bis(dodecyloxy)benzene (3): White solid. (16g, 84%) ^{1}H NMR (400 MHz, $CDCl_3$): δ 6.84(s, 4H), 3.91(t, J3=8Hz, 2H) 1.28-1.80(m, 41H), 0.88-0.91(m, 6H).

Synthesis of 1,4-bis(bromomethyl)-2,5-bis(dodecyloxy)benzene (4): In a two necked round bottom flask, compound **3** (1.45g, 3.30mmol), paraformaldehyde (0.21g, 7mmol) in acetic acid (20 mL) and HBr (1.40 mL) was added in one portion. The reaction mixture was heated at 80 ℃ for 12h. After the completion of reaction, the reaction mixture was poured in to water and extracted with chloroform. Combined organic phase was washed with water, dried over anhydrous sodium sulphate, concentrated under reduced pressure and crude product was purified by column chromatography over silica gel. The pure product was eluted using 10% ethyl acetate- petroleum ether as mobile phase.

1,4-Bis(bromomethyl)-2,5-bis(dodecyloxy)benzene (4): White solid. (1.33g, 83%); ^{1}H NMR (400 MHz, $CDCl_3$): δ 6.85(s, 2H), 4.52(s, 4H), 3.98(t, J3=8 Hz, 4H), 1.86-1.28(m, 40H) 0.88-0.91(m, 6H).

Synthesis of (2,5-bis(dodecyloxy)-1,4-phenylene)bis(methylene) diacetate (5): In a two-necked round bottom flask compound **4** (2.2g, 3.4mmol), potassium acetate (1.03g, 10.4mmol) and tetra n-butyl ammonium bromide (0.17g, 0.26mmol) in chloroform (25 mL) and acetonitrile (50ml) was added and the reaction mixture was allowed to refluxed for 12h. After cooling to room temperature, the resulting mixture was poured in to 200 mL of water and extracted with chloroform. The combined organic layer was washed with water and dried over anhydrous sodium sulphate. The pure product was obtained by removal of solvent under reduced pressure.

2,5-Bis(dodecyloxy)-1,4-phenylene)bis(methylene) diacetate (5): Colourless solid (1.95g, 100%). ^{1}H NMR (400 MHz, $CDCl_3$): δ 6.88 (s, 2H), 5.14 (s, 4H), 3.94 (t, J2=12Hz, 4H), 1.21-2.01 (m, 21H), 0.88-0.91 (m, 3H).

Synthesis of (2,5-bis(dodecyloxy)-1,4-phenylene)dimethanol (6): Compound **5** (1.95g ,5.62mmol) and lithium aluminium hydride ($LiAlH_4$) (0.85g, 22.4mmol) was added in dry THF under nitrogen atmosphere and the reaction mixture was stirred at room temperature for 2h. After completion of the reaction, excess of $LiAlH_4$ was quenched by ethyl acetate at 0 ℃ and the resulting mixture was poured in to water and extracted with chloroform. The combined organic layer was washed with water and dried over anhydrous sodium sulphate. The pure product was obtained by removal of solvent under reduced pressure.

(2,5-Bis(dodecyloxy)-1,4-phenylene)dimethanol (6): Colourless solid. (1.52g, 98%) ^{1}H NMR (400 MHz, $CDCl_3$): δ 6.88 (s, 2H), 5.14 (s, 4H), 3.94 (t, J2=12Hz, 4H), 1.21-2.10 (m, 20H), 0.88-0.91 (m, 4H).

Synthesis of 2,5-bis(hydroxymethyl)benzene-1,4-dialdehyde (7): Compound **6** (1.52g, 3.04mmol) and pyridinium chlorochromate (PCC) (2.49g, 11.5mmol) was added in 20 mL dichloromethane (DCM) and the reaction mixture was stirred for 2h at room temperature. After completion of reaction, the reaction mixture was directly added on the silica gel column and the product was obtained with high fluorescence.

2,5-Bis(hydroxymethyl)benzene-1,4-dialdehyde (7): (1.27g, 90%) ^{1}H NMR (400 MHz, $CDCl_3$): δ 10.53 (s, 2H), 7.43 (s, 2H), 4.07 (t, J3=12Hz, 4H), 1.27-1.87 (m, 21H), 0.87-0.90 (m, 3H).

Synthesis of monomers

Synthesis of (3Z,3'Z)-3,3'-(1,4-phenylenebis(methaneylylidene)) bis(5-bromo-1-tetradecylindolin-2-one) (TIIG): In 22 mL of absolute ethanol, terephthalaldehyde (0.041g, 0.30mmol) and compound **2** (0.20g, 0.16mmol) are added under nitrogen atmosphere. To this stirred solution, piperidine (0.1 mL, 1.07mmol) is added dropwise and the reaction mixture was reflux for 24h. After that, reaction mixture is cooled to room temperature and the precipitated product is collected by filtration. The filtered product was washed with copious amount of absolute ethanol and dried at room temperature. The pure product was obtained by re-crystallization from petroleum ether-chloroform solution.

(*3Z,3′Z*)-3,3'-(1,4-Phenylenebis(methaneylylidene))bis(5-bromo-1-tetradecylindolin-2-one) (TIIG): Dark orange solid (0.14g, 65%) ^{1}H NMR (400 MHz, $CDCl_3$): 8.38 (s, 2H), 7.64 (d, J3 = 2.0 Hz, 1H), 7.49 (s, 1H), 7.36 (dd, J2 = 8.0 Hz, J3 = 1.6 Hz, 1H), 6.68 (d, J2 = 8.4 Hz, 1H), 3.69−3.73 (t, J2 = 7.6 Hz, 2H), 1.68−1.73 (m, 2H), 0.95−0.98 (t, J2 = 7.6 Hz, 3H). ^{13}C NMR (100 MHz, $CDCl_3$): δ 165.3, 140.9, 137.1, 135.6, 132.2, 131.5, 126.2, 122.4, 114.4, 109.6, 40.1, 31.9, 29.5, 29.3, 27.5, 22.7, 14.1. HRMS(ES$^+$): $C_{52}H_{71}N_2O_2Br_2$ requires 913.3876, found 913.3882 IR (KBr, cm^{-1}): 3128.88, 3081.83, 2919.86, 2850.21, 1692.34, 1599.53, 1468.44, 1365.61, 1303.08, 1206.51, 1169.24, 1109.92, 867.04, 777.53, 677.20, 608.35.

Synthesis of (3Z,3'Z)-3,3'-((2,5-bis(dodecyloxy)-1,4-phenylene) bis(methaneylylidene)) bis(5-bromo-1-tetradecylindolin-2-one) (DAB): To a 100 mL round bottom flask; compound **7** (0.35g, 0.61mmol) and compound **2** (0.5g, 1.22mmol)) in acetonitrile (15mL) and chloroform (15 mL) are added and stir at room temperature. The reaction mixture was degassed by purging nitrogen gas. To this stirred solution piperidine (0.18g, 2.13mmol) was added dropwise and the reaction mixture was allowed to reflux for 24h. After that, reaction mixture is cooled to room temperature and the precipitated product is collected by filtration. The filtered product was washed with copious amount of acetonitrile and dried at room temperature. The pure product was obtained by re-crystallization from petroleum ether-chloroform solution.

(*3Z,3′Z*)-3,3'-((2,5-Bis(dodecyloxy)-1,4-phenylene)bis(methaneylylidene))bis(5-bromo-1-tetradecylindolin-2-one) (DAB): Dark red solid (0.5g, 75%), ^{1}H NMR (400MHz, $CDCl_3$) δ: 8.81 (s, 2H), 8.01 (s, 2H) 7.60 (d, J3=4.0 Hz, 1H) 7.34 (dd, J2=8.0 Hz, 1H), 6.66 (d, J2=8Hz, 1H), 4.18 (t, J2=8Hz 2H), 3.71 (d, J2=8Hz), 1.57 (m, 6H), 1.24-1.32 (m, 41H), 0.84-0.87 (m, 9H), ^{13}C NMR (100 MHz, $CDCl_3$): δ 165.7, 152.1, 140.4, 131.8, 131.0, 127.0, 126.8, 124.8, 122.3, 115.1, 114.3, 109.3, 40.0, 31.9, 29.7, 26.6, 22.12, 14.16. MALDI-TOF (ES$^+$): $C_{76}H_{119}Br_2N_2O_4$ requires 1228.49 found 1228.59 IR (KBr, cm^{-1}): 3470.73, 2921.21, 2851.43, 1714.69, 1607.92, 1457.37, 1390.50, 1339.35, 1111.16, 1033.27, 865.30, 800.29, 636.67.

Synthesis of (3Z,3'Z)-3,3'-(thiophene-2,5-diylbis(methaneylylidene)bis(5-bromo-1-tetradecylindolin-2-one) (THP): To a 100 mL round bottom flask, thiophene-2,5-dicarboxyaldehyde (0.12g, 0.85mmol) and compound **2** (0.7g,

1.75mmol) in acetonitrile (15mL) and chloroform(15mL) are stirred at room temperature. The reaction mixture is degassed by purging nitrogen gas. To this stirred solution piperidine (0.25g, 3.0mmol) was added dropwise and the reaction mixture was allowed to reflux for 24h. After that, the reaction mixture is cooled to room temperature and the precipitated product is collected by filtration. The filtered product was washed with copious amount of acetonitrile and dried at room temperature The pure product was obtained by re-crystallization from petroleum ether-chloroform solution.

(*3Z,3'Z*)-3,3'-(Thiophene-2,5-diylbis(methaneylylidene))bis(5-bromo-1-tetradecylindolin-2-one) (THP): Brown solid (0.64g, 70%), ^{1}H NMR (400 MHz, $CDCl_3$) δ: 8.09 (s, J2=16Hz, 1H), 7.90 (s, 1H), 7.53 (s, 1H), 7.53 (dd, J3=8Hz,1H), 7.2 (s, 1H), 6.65 (dd, J3=8Hz, 1H), 3.75 (d J2=12Hz, 2H), 1.60-1.69 (d, 3H), 1.07-1.33 (m, 23H), 0.70-0.87 (d, 3H), ^{13}C NMR (100 MHz, $CDCl_3$): δ 143.8, 140.6, 137.1, 131.4d, 127.7, 125.6, 122.1, 114.3, 109.6, 40.1, 31.9, 29.7, 29.6, 29.5, 29.3, 27.6, 22.7. HRMS(ES^+): $C_{50}H_{69}N_2O_2Br_2S$ requires 919.3421, found 919.3447. IR (KBr, cm^{-1}): 3098.39, 2962.30, 2919.83, 2850.36, 1693.61, 1591.51, 1433.57, 1378.10, 1261.25, 1186.41, 1142.82, 1021.92, 801.00, 707.97, 665.58

Synthesis of polymers

5,5'-Bis(trimethylstannyl)-2,2'-bithiophene is coupled with corresponding π-extended isoindigo compounds, **TIIG, DAB** and **THP** using $Pd_2(dba)_3$ and tri-*o*-tolylphosphine as the catalyst-ligand system in refluxing toluene. The detailed experimental procedure for polymerization is mentioned below.

General procedure for synthesis of iso-indigo based polymers TIIG-P, DAB-P and THP-P

To an oven dried, two-necked round bottom flask **TIIG** (0.2 g, 0.20 mmol, 1eq), **DAB** (0.3 g, 0.20 mmol, 1eq) or **THP** (0.3 g, 0.30 mmol, 1eq) and 5,5'-bis(trimethylstannyl)-2,2'bithiophene (1.05 eq) was added. To this $Pd_2(dba)_3$ (0.05 mole %), tri-*o*-tolylphosphine (0.21 mole%) and 20 mL of anhydrous toluene was added under nitrogen atmosphere. The resulting solution was degassed by purging nitrogen for 20 minutes. The reaction mixture is then heated at 120 ℃ for 72h. After that 2-bromo thiophene (0.1 mL) was added and the reaction mixture was stirred for 2h. After completion of the reaction, the reaction mixture was cool to room temperature, toluene

was evaporated under vacuum and precipitate was collected by adding methanol. The resulting precipitate were filtered and washed with methanol. Obtained crude polymers are subjected to Soxhlet extraction using methanol, acetone, pet ether and chloroform. The polymers were obtained by evaporation of chloroform fraction under reduced pressure and further dried under vacuum at 50 ℃ to yield corresponding polymers.

TIIG-P: Reddish-orange colour polymer. ^{1}H NMR (400MHz, $CDCl_3$): δ 8.43 (br s, 1H), 8.12 (br s, 2H), 7.36 (br s, 3H), 7.17 (br s, 2H), 6.70 (br s, 2H), 3.77 (br s, 3H), 1.26 (37H), 1.20 (6H). IR (KBr, cm^{-1}): 3433.89, 3064.41, 2922.11, 2850.57, 1697.01, 1611.02, 1483.22, 1461.84, 1435.14, 1263.04, 1168.78, 1112.15, 915.70, 874.50, 696.23, 527.98.

DAB-P: Dark red polymer. ^{1}H NMR (400 MHz, $CDCl_3$): δ 8.80 (br s, 1H), 8.10 (br s, 1H), 7.64 (br s, 2H), 7.37 (br s, 1H), 6.70 (br s, 2H), 4.21 (br s, 3H), 3.75 (br s, 3H), 1.88 (br s, 5H), 1.26 (br s, 6H), 0.87 (br s, 15H). IR (KBr, cm^{-1}): 3433.98, 2920.17, 2850.75, 1678.15, 1607.90, 1501.59, 1476.03, 1392.01, 1375.35, 1265.39, 1255.08, 1139.28, 1111.34, 1036.98, 927.95,797.52, 675.12, 542.47.

THP-P: Brown coloured polymer. ^{1}H NMR (400 MHz, $CDCl_3$): δ 8.21 (br s, 1H), 6.85 (br s, 7h), 3.76 (br s, 2H), 0.88 (br s, 32H). IR (KBr, cm^{-1}): 3442.88, 2929.94, 2849.89, 1691.52, 1609.64, 1481.35, 1459.34, 1367.22, 1259.77, 1166.75, 1111.17, 1034.14, 899.80, 869.99, 718.58, 669.91, 530.99, 441.97.

Spectral data

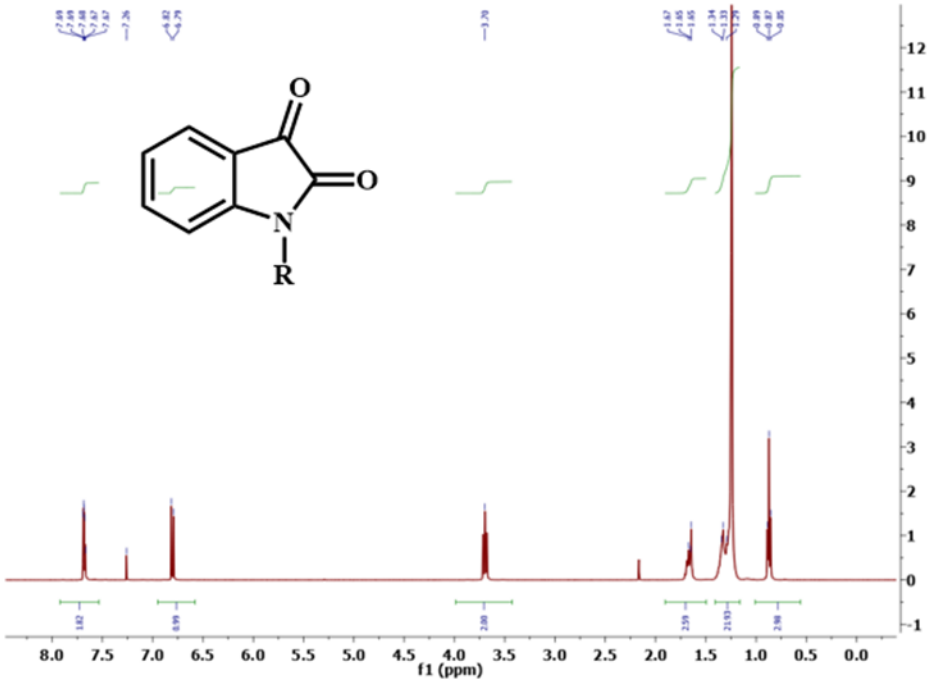

Figure 2.16 ^{1}H NMR spectra of compound **1**

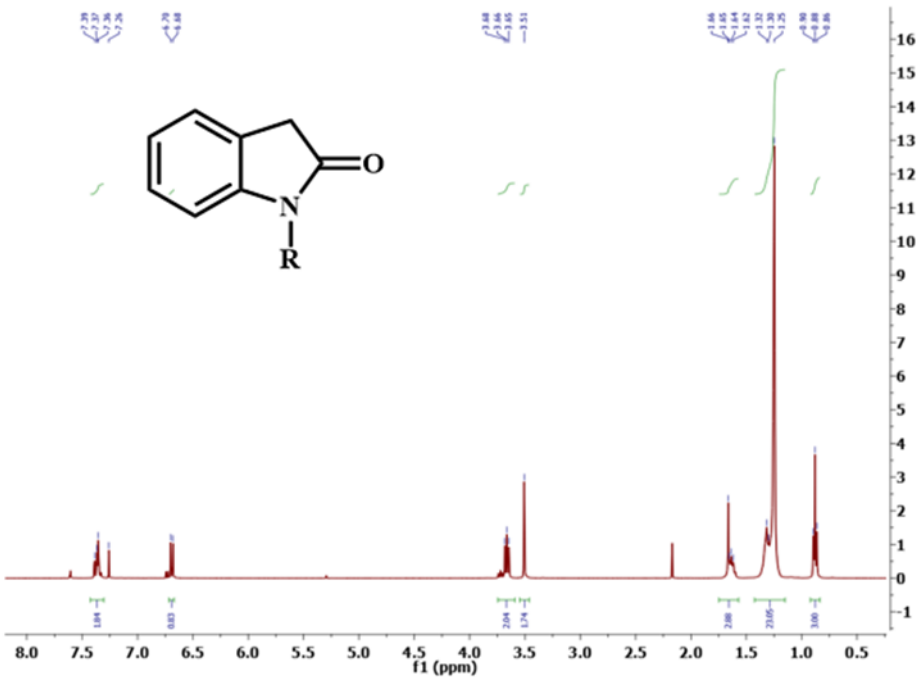

Figure 2.17 ^{1}H NMR spectra of compound **2**

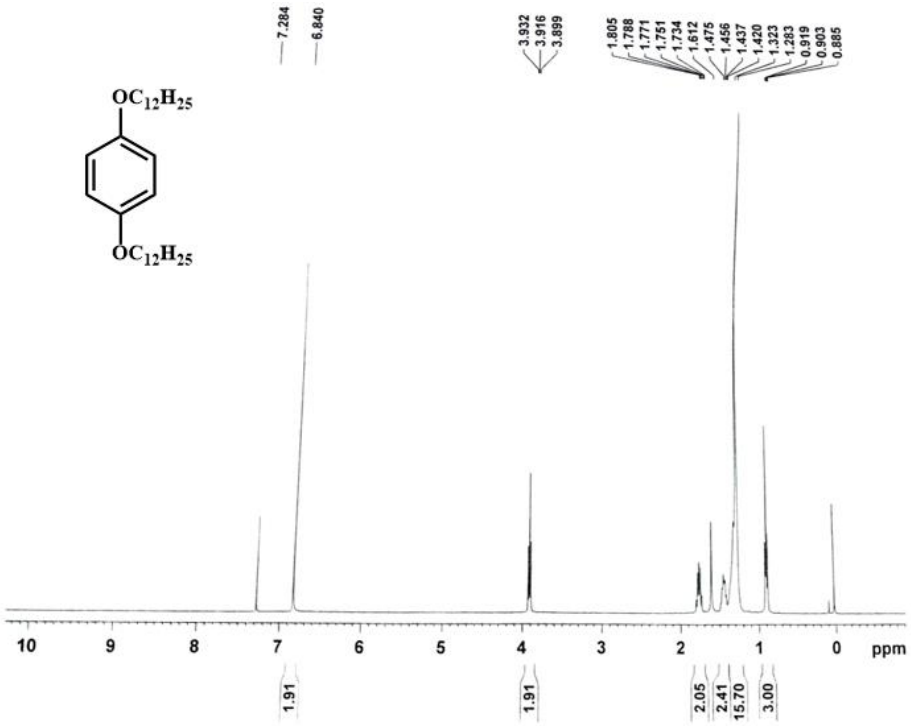

Figure 2.18 ^{1}H NMR spectra of compound **3**

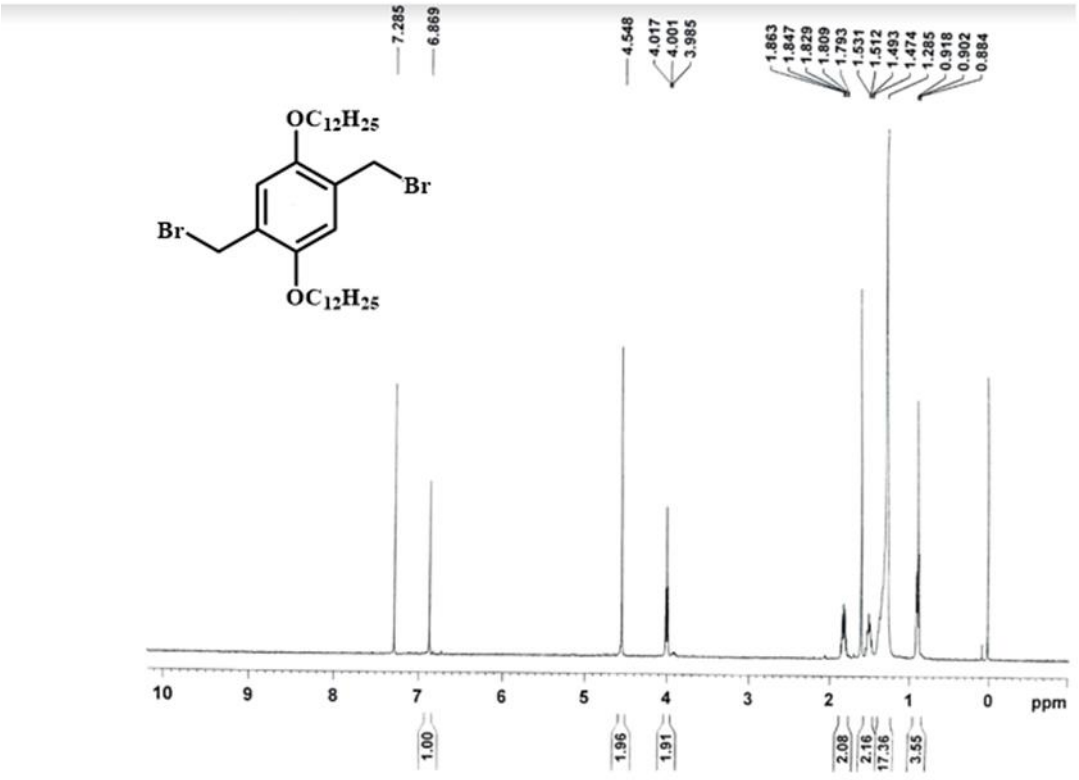

Figure 2.19 ^{1}H NMR spectra of compound **4**

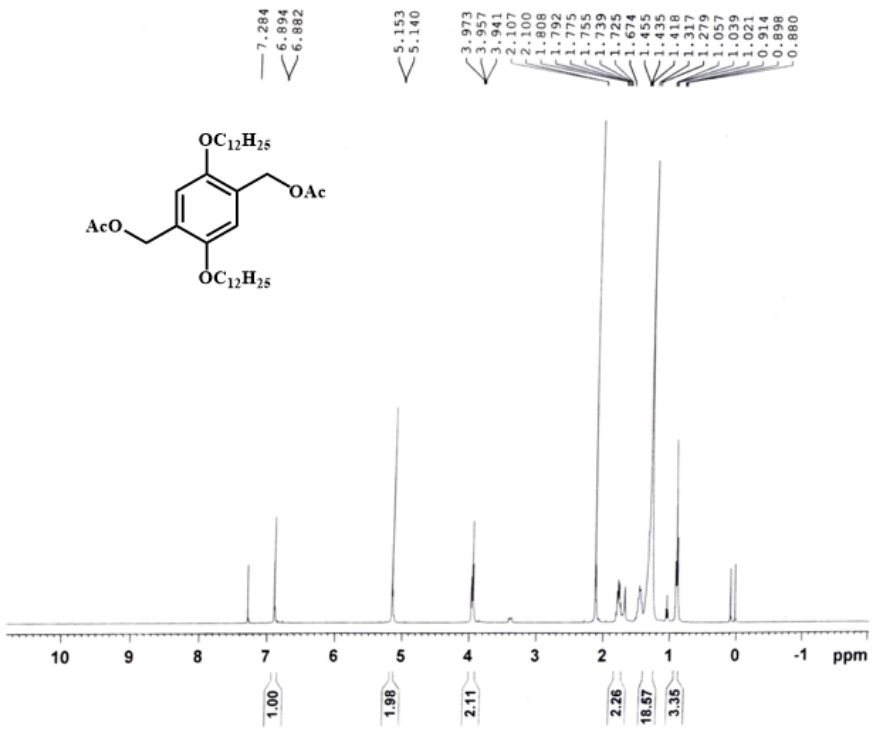

Figure 2.20 ^{1}H NMR spectra of compound **5**

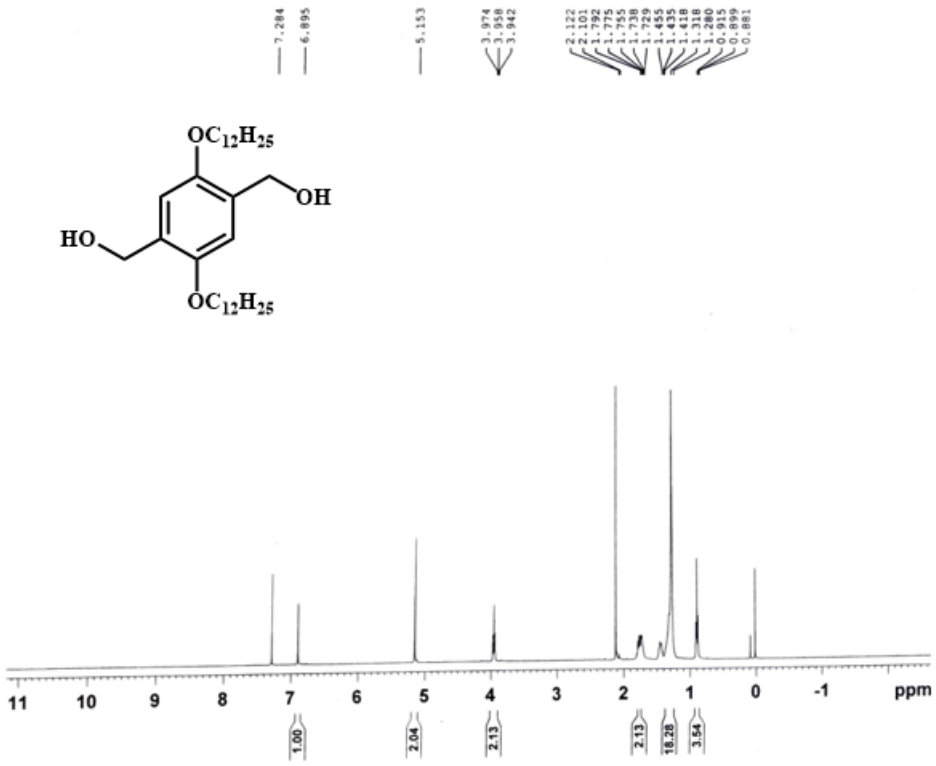

Figure 2.21 ^{1}H NMR spectra of compound **6**

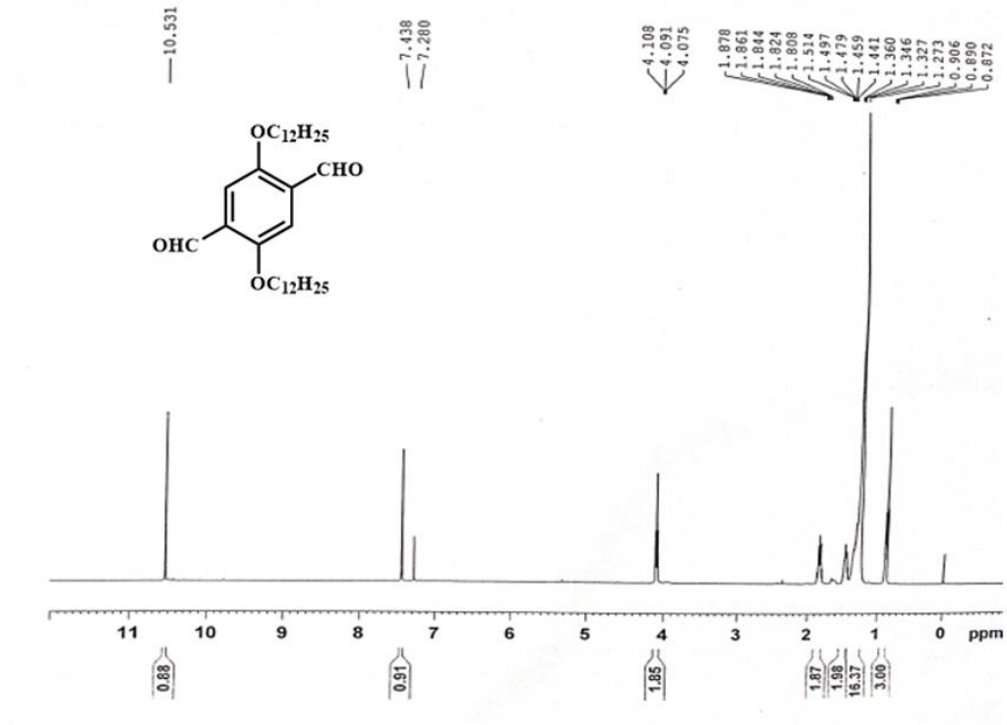

Figure 2.22 ^{1}H NMR spectra of compound **7**

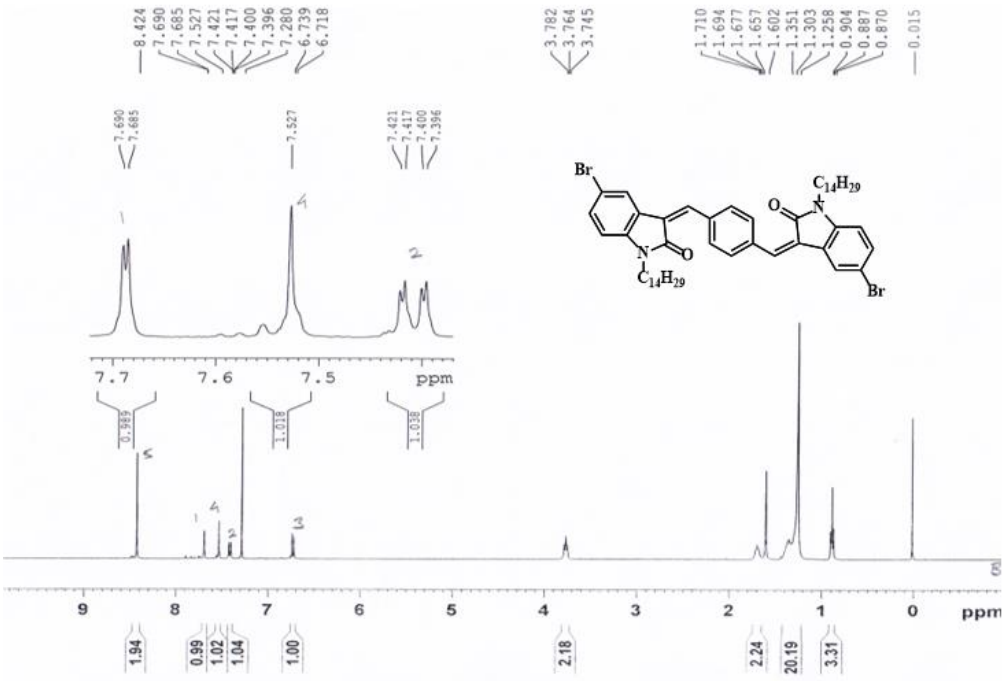

Figure 2.23 ^{1}H NMR spectra of **TIIG**

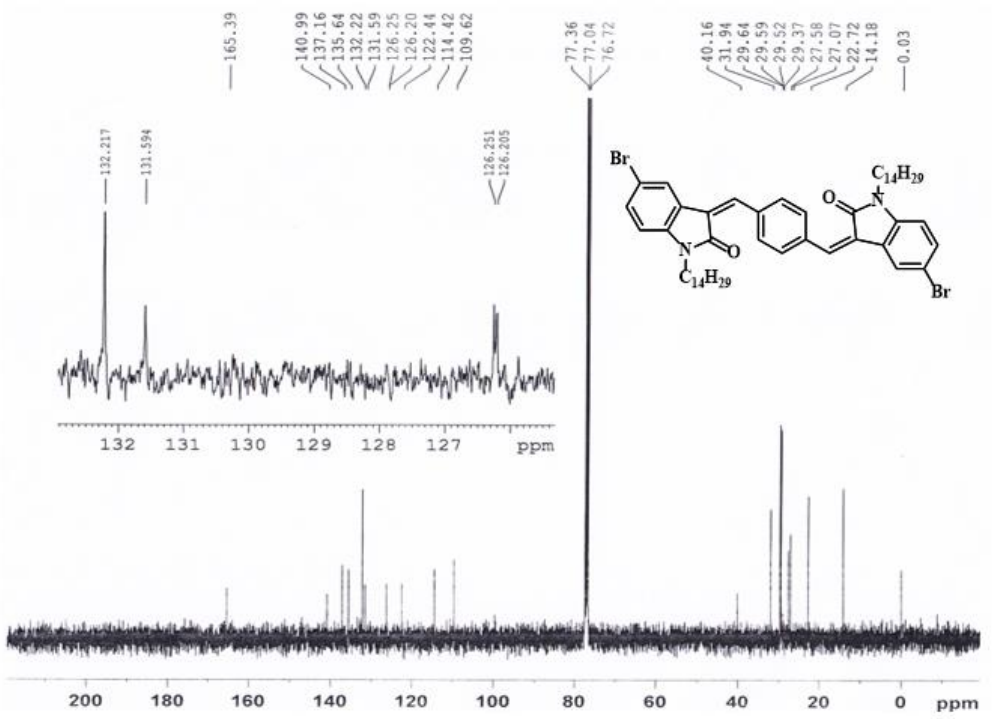

Figure 2.24 ^{13}C NMR spectra of **TIIG**

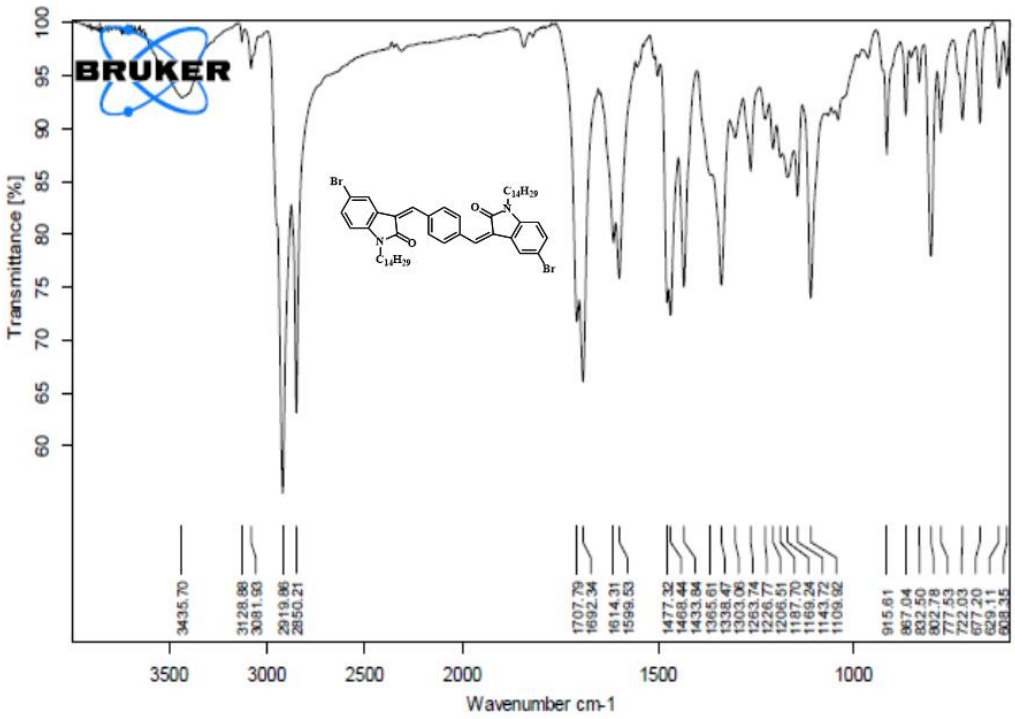

Figure 2.25 IR spectra of **TIIG**

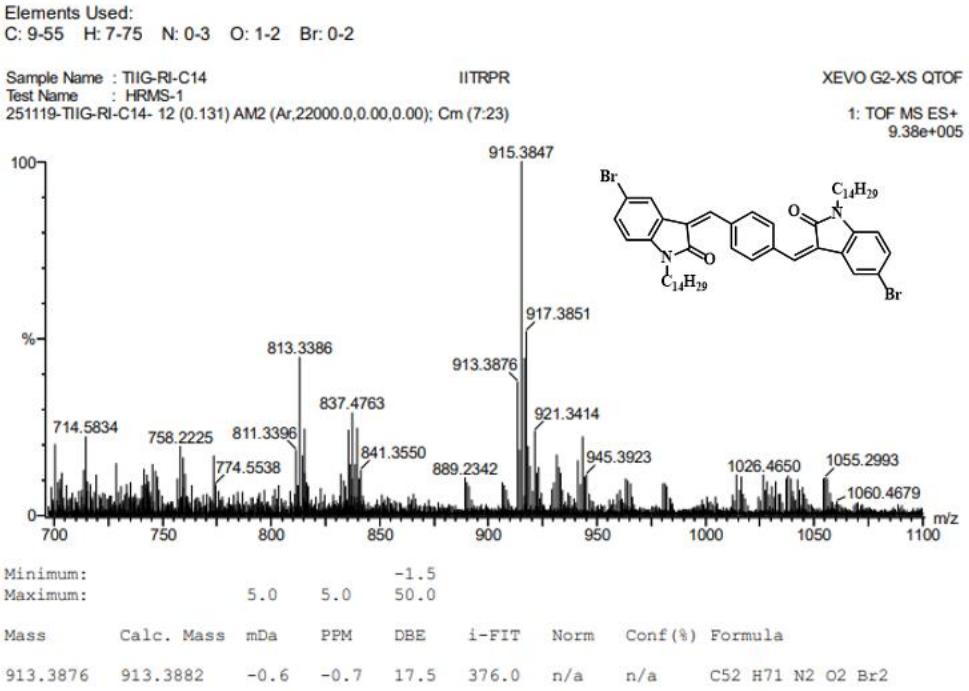

Figure 2.26 HR-MS DATA of **TIIG**

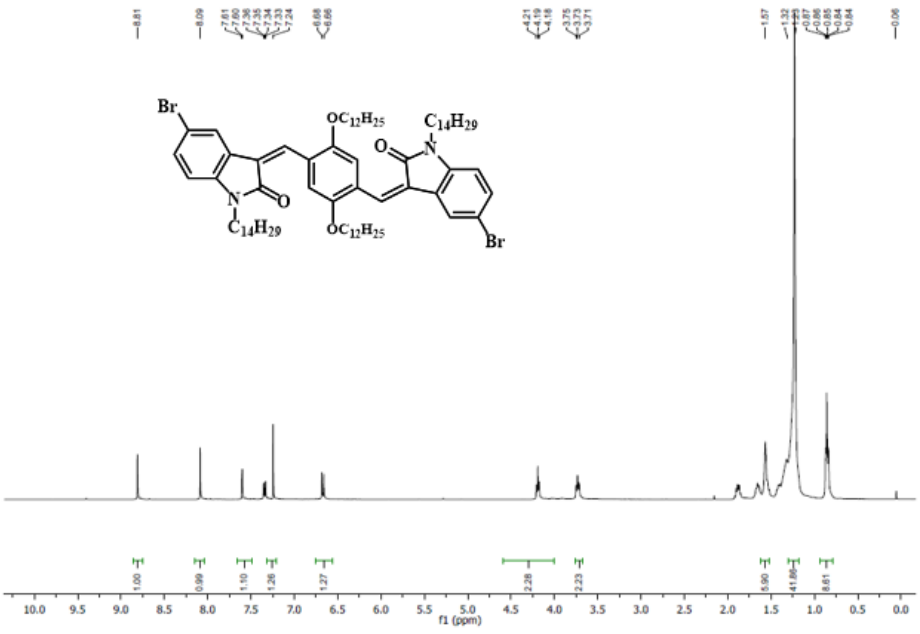

Figure 2.27 ^{1}H NMR spectra of **DAB**

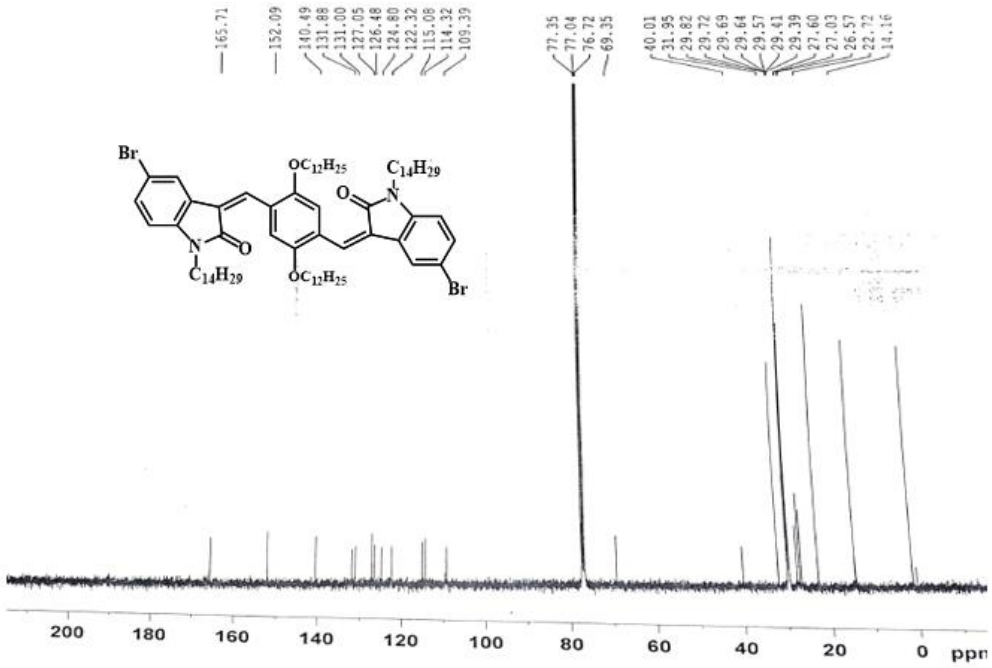

Figure 2.28 ^{13}C NMR spectra of **DAB**

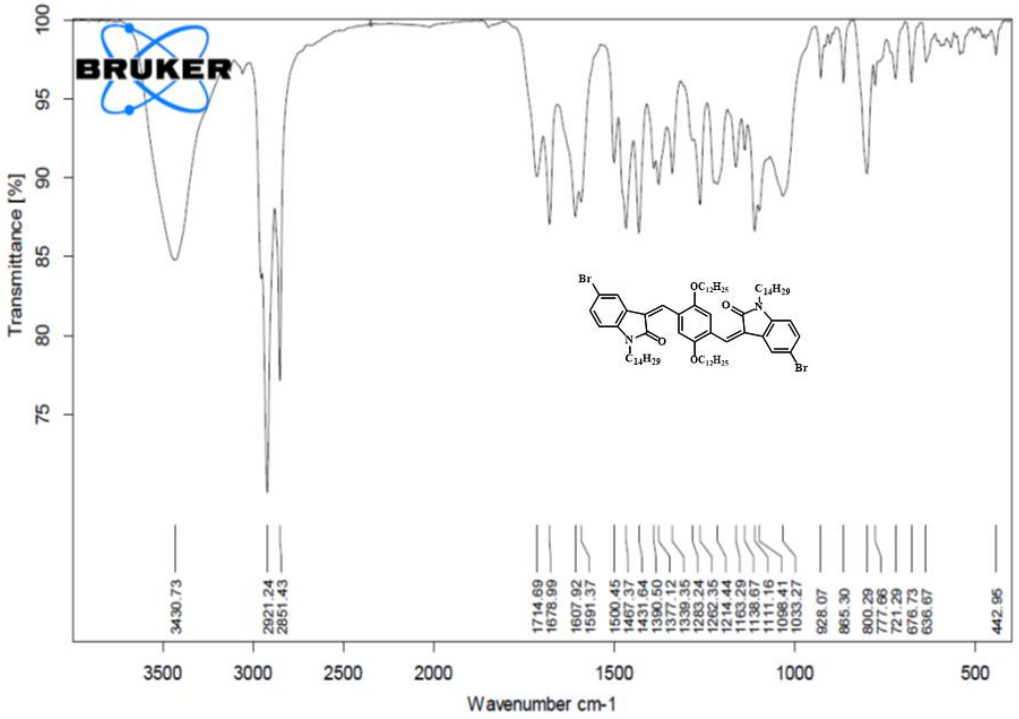

Figure 2.29 IR spectra of **DAB**

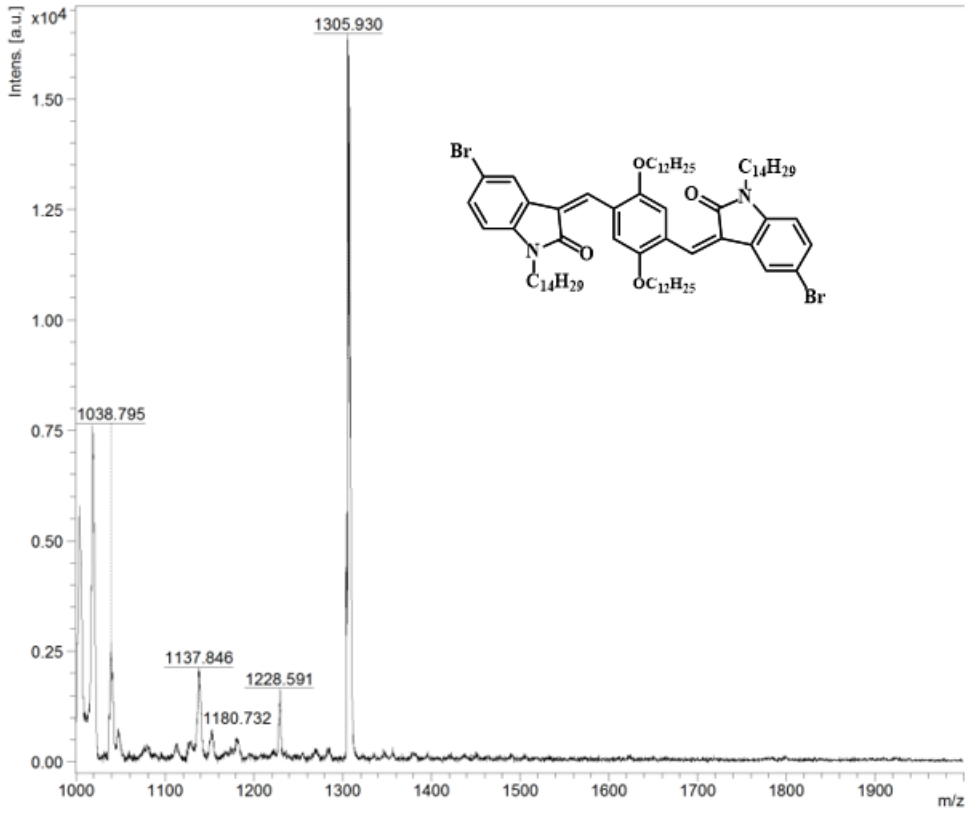

Figure 2.30 MALDI-TOF spectra of DAB

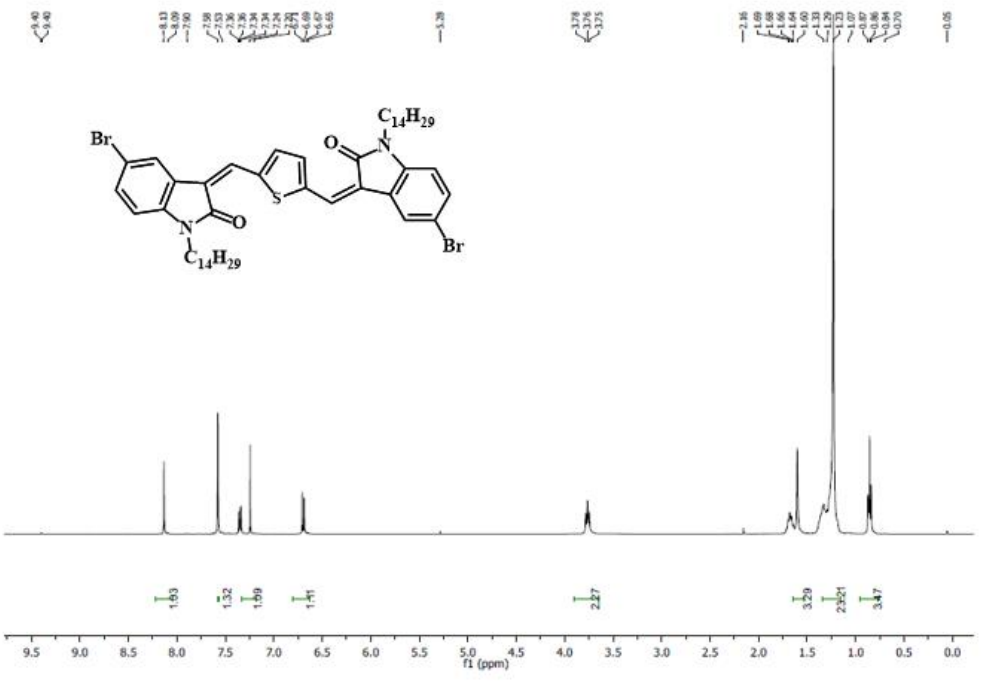

Figure 2.31 ^{1}H NMR spectra of **THP**

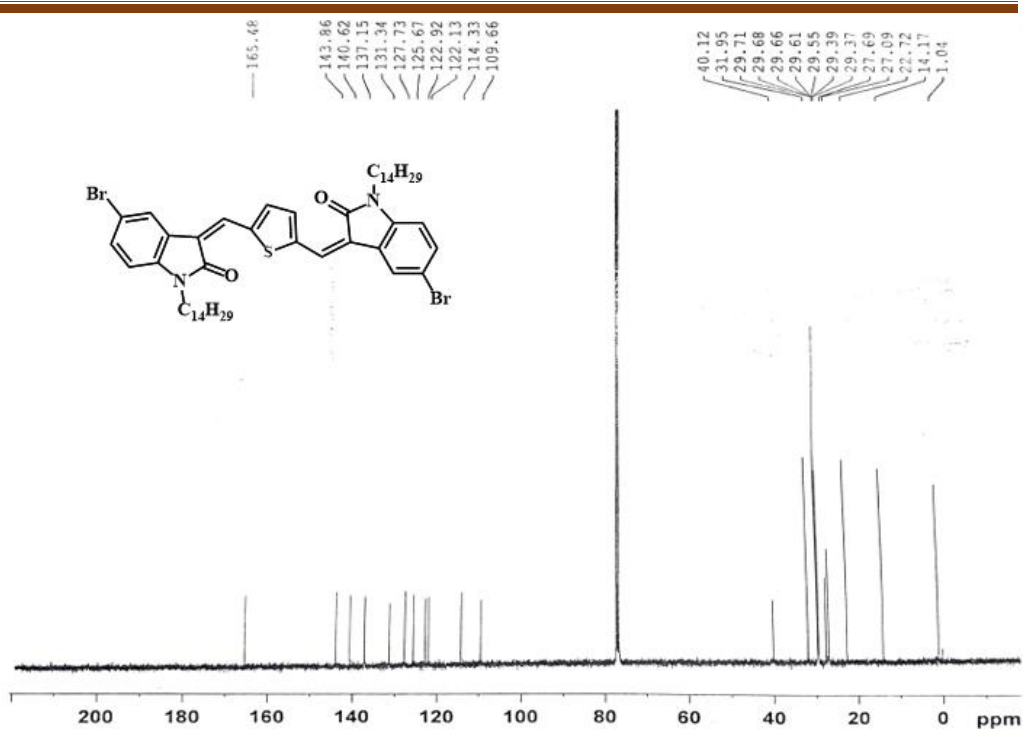

Figure 2.32 ^{13}C NMR spectra of **THP**

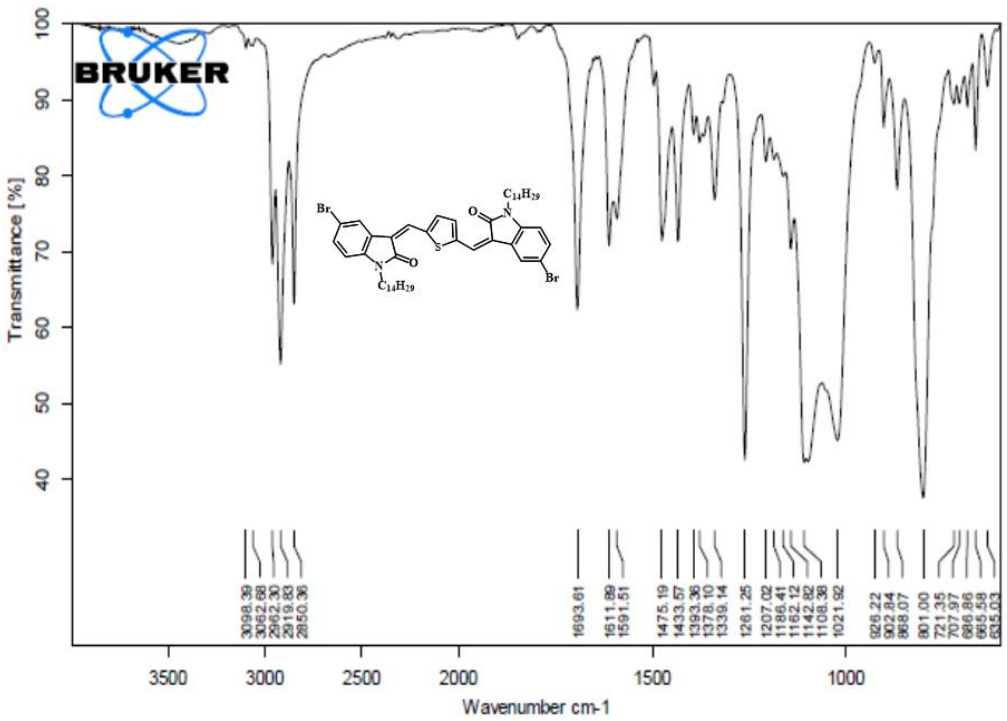

Figure 2.33 IR spectra of **THP**

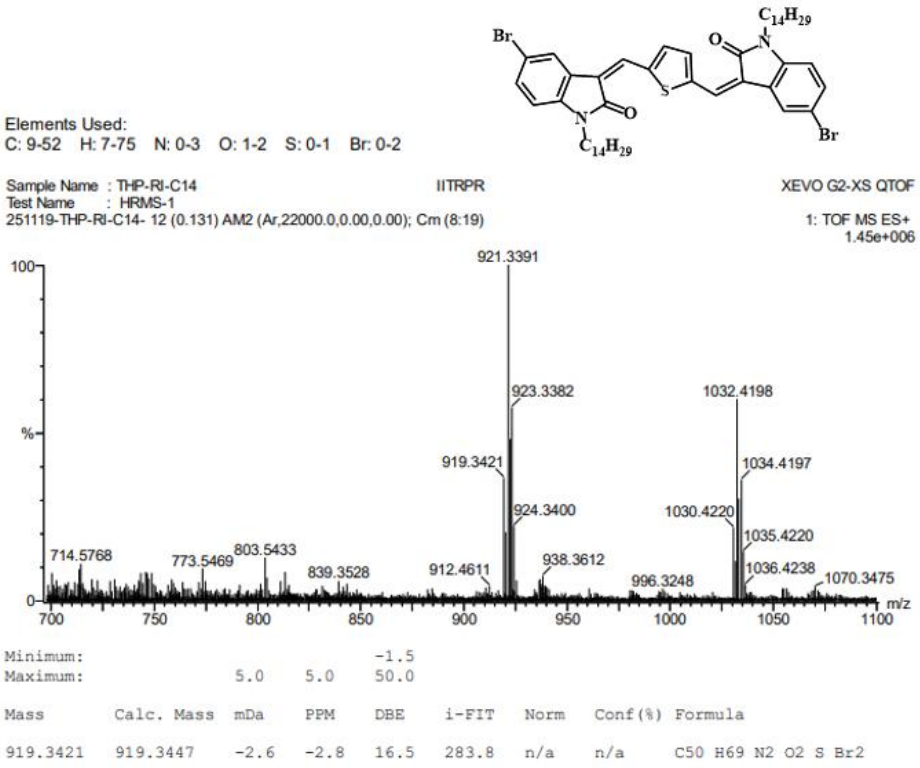

Figure 2.34 HR-MS DATA of **THP**

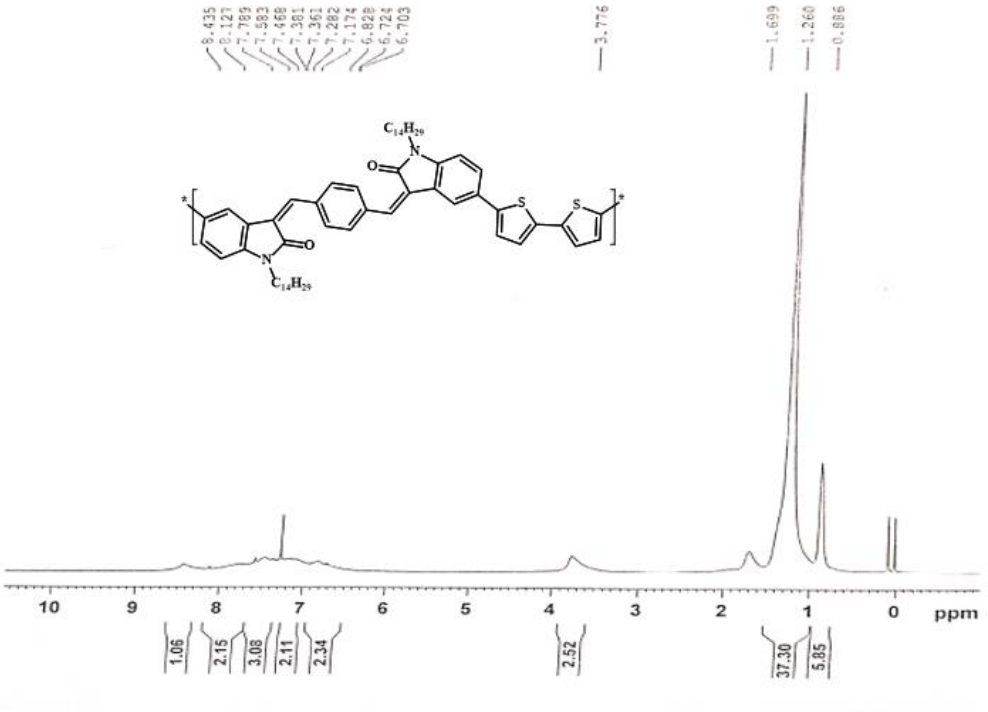

Figure 2.35 ^{1}H NMR spectra of **TIIG-P**

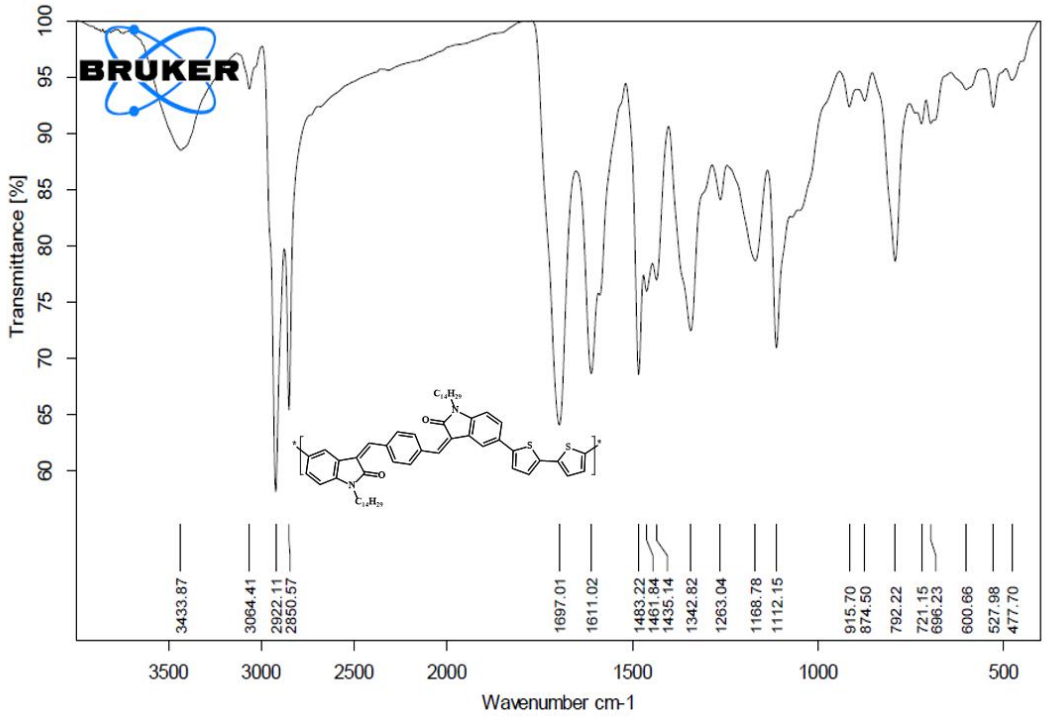

Figure 2.36 IR spectra of **TIIG-P**

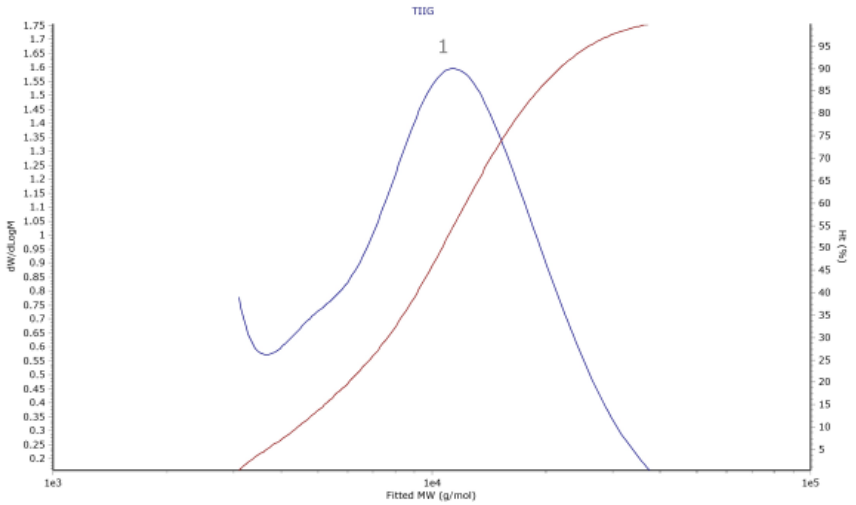

Results

Analysed by
Comments

Applied Chem at 16:53:44 on 17 November 2021

Molecular Weight Averages

Peak	Mp (g/mol)	Mn (g/mol)	Mw (g/mol)	Mz (g/mol)	Mz+1 (g/mol)	Mv (g/mol)	PD
Peak 1	11475	8672	12054	15978	19808	15405	1.39

Figure 2.37 GPC analysis report of **TIIG-P**

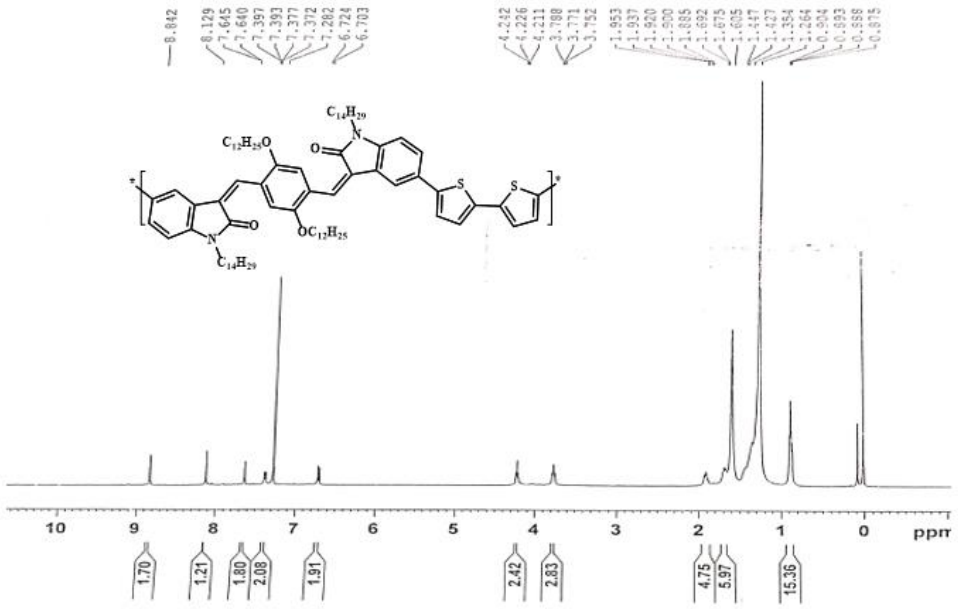

Figure 2.38 ^{1}H NMR spectra of **DAB-P**

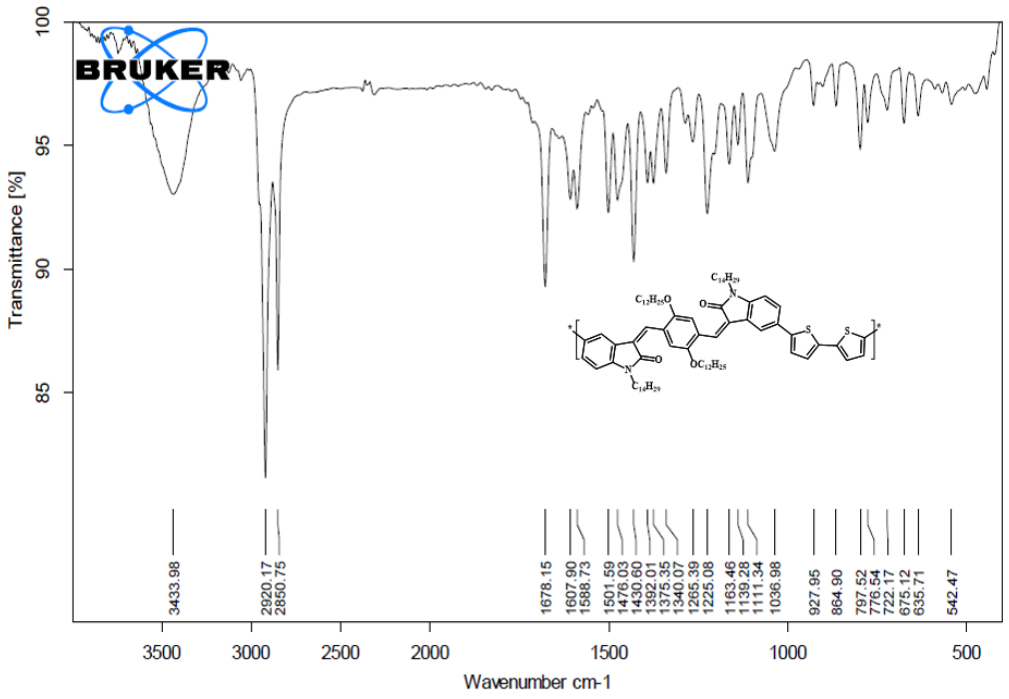

Figure 2.39 IR spectra of **DAB-P**

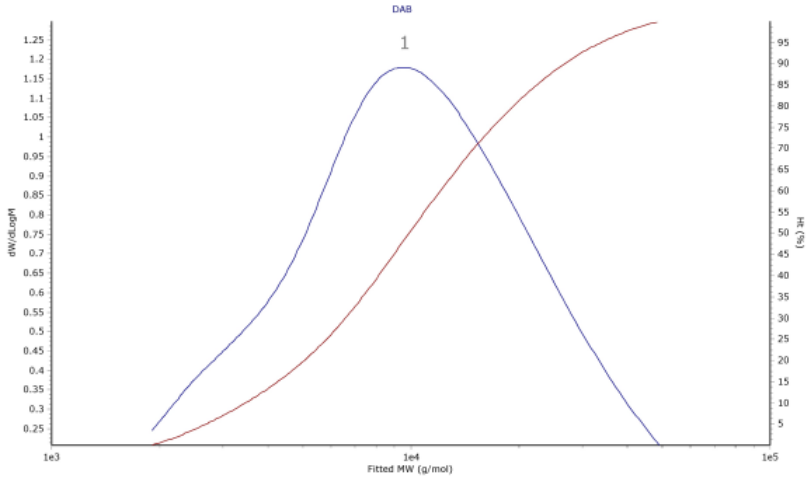

Results

Analysed by
Comments

Applied Chem at 16:36:24 on 17 December 2019

Molecular Weight Averages

Peak	Mp (g/mol)	Mn (g/mol)	Mw (g/mol)	Mz (g/mol)	Mz+1 (g/mol)	Mv (g/mol)	PD
Peak 1	9788	7458	12827	20095	27033	19037	1.72

Figure 2.40 GPC analysis report of **DAB-P**

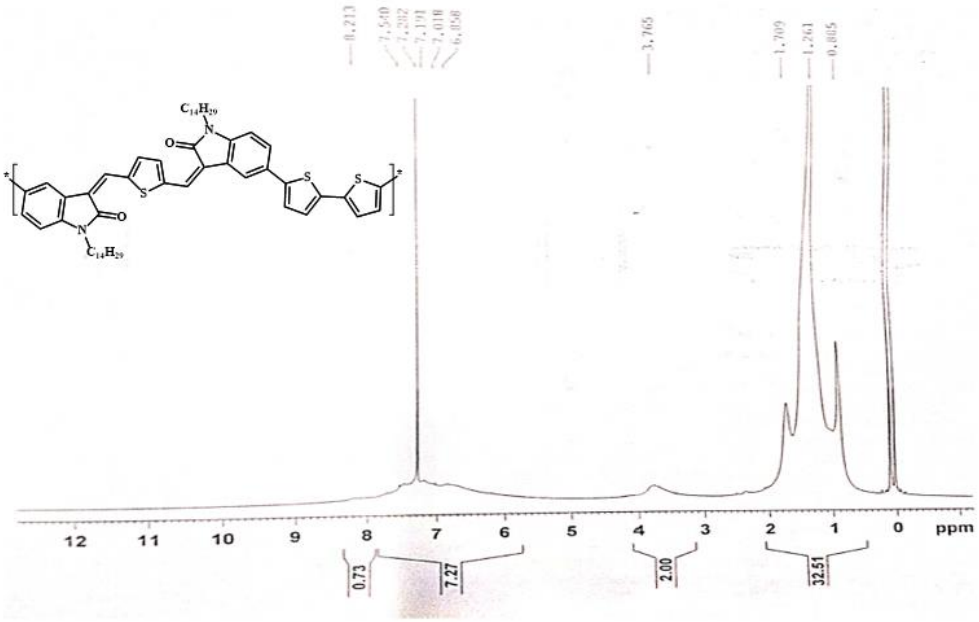

Figure 2.41 ^{1}H NMR spectra of **THP-P**

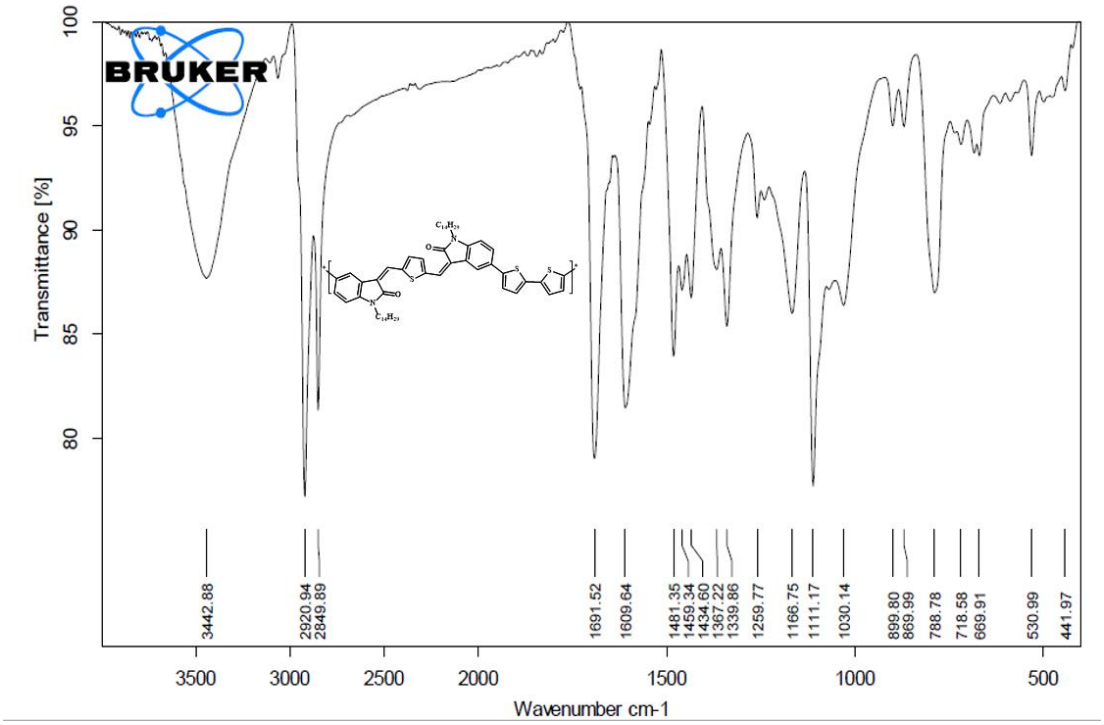

Figure 2.42 IR spectra of **THP-P**

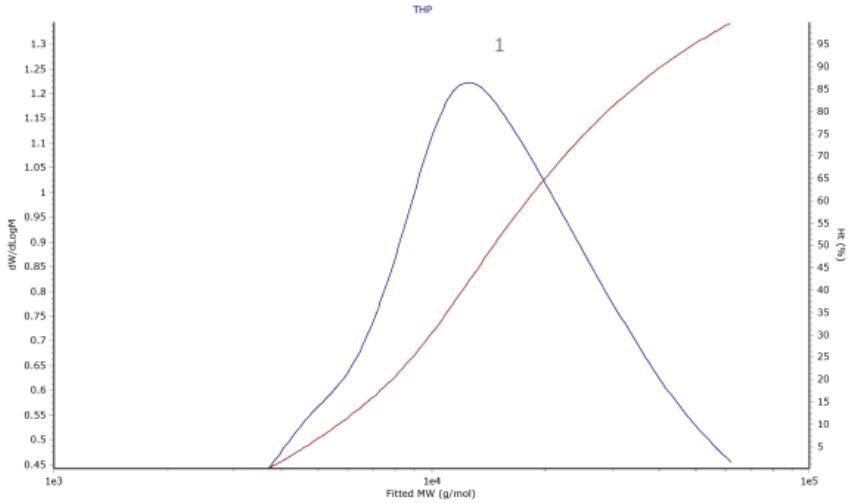

Results

Analysed by: Applied Chem at 17:03:19 on 17 November 2021

Comments

Molecular Weight Averages

Peak	Mp (g/mol)	Mn (g/mol)	Mw (g/mol)	Mz (g/mol)	Mz+1 (g/mol)	Mv (g/mol)	PD
Peak 1	12734	11793	19091	28902	37759	27502	1.619

Figure 2.43 GPC analysis report of **THP-P**

References

1 Y. Liu, F. Wu, B. Zhao and P. Shen, *Eur. Polym. J.*, 2016, **74**, 180–189.

2 S. I. Kato, T. Furuya, A. Kobayashi, M. Nitani, Y. Ie, Y. Aso, T. Yoshihara, S. Tobita and Y. Nakamura, *J. Org. Chem.*, 2012, **77**, 7595–7606.

3 S. Ghosh, S. Das, N. R. Kumar, A. R. Agrawal and S. S. Zade, *New J. Chem.*, 2017, **41**, 11568–11575.

4 S. Ren, W. Zhang, Z. Wang, A. Yassar, Z. Liao and Z. Yi, *Polymers (Basel).*,2023, **15**, 3803-3816.

5 C. Wang, H. Dong, W. Hu, Y. Liu and D. Zhu, *Chem. Rev.*, 2012, **112**, 2208–2267.

6 L. Lu, T. Zheng, Q. Wu, A. M. Schneider, D. Zhao and L. Yu, *Chem. Rev.*, 2015, **115**, 12666–12731.

7 L. Shi, Y. Guo, W. Hu and Y. Liu, *Mater. Chem. Front.*, 2017, **1**, 2423–2456.

8 S. Ren, Y. Ding, W. Zhang, Z. Wang, S. Wang and Z. Yi, *Polymers (Basel).*, 2023, **15**, 3803.

9 W. J. Jeong, K. Lee, J. Jang and I. H. Jung, *Polymers (Basel).*, 2023, **15**, 1156-1171.

10 B. S. Ong, Y. Wu, P. Liu and S. Gardner, *J. Am. Chem. Soc.*, 2004, **126**, 3378–3379.

11 W. Zhang, J. Smith, S. E. Watkins, R. Gysel, M. McGehee, A. Salleo, J. Kirkpatrick, S. Ashraf, T. Anthopoulos, M. Heeney and I. McCulloch, *J. Am. Chem. Soc.*, 2010, **132**, 11437–11439.

12 Q. Liu, C. Li, E. Jin, Z. Lu, Y. Chen, F. Li and Z. Bo, *ACS Appl. Mater. Interfaces*, 2014, **6**, 1601–1607.

13 N. Blouin, A. Michaud, D. Gendron, S. Wakim, E. Blair, R. Neagu-Plesu, M. Belletête, G. Durocher, Y. Tao and M. Leclerc, *J. Am. Chem. Soc.*, 2008, **130**, 732–742.

14 H. H. Fong, V. A. Pozdin, A. Amassian, G. G. Malliaras, D.-M. Smilgies, M.

He, S. Gasper, F. Zhang and M. Sorensen, *J. Am. Chem. Soc.*, 2008, **130**, 13202–13203.

15 M. Zhang, X. Guo, X. Wang, H. Wang and Y. Li, *Chem. Mater.*, 2011, **23**, 4264–4270.

16 I. McCulloch, M. Heeney, C. Bailey, K. Genevicius, I. MacDonald, M. Shkunov, D. Sparrowe, S. Tierney, R. Wagner, W. Zhang, M. L. Chabinyc, R. J. Kline, M. D. McGehee and M. F. Toney, *Nat. Mater.*, 2006, **5**, 328–333.

17 M. Zhang, H. N. Tsao, W. Pisula, C. Yang, A. K. Mishra and K. Müllen, *J. Am. Chem. Soc.*, 2007, **129**, 3472–3473.

18 J. Liu, R. Zhang, G. Sauvé, T. Kowalewski and R. D. McCullough, *J. Am. Chem. Soc.*, 2008, **130**, 13167–13176.

19 V. J. Bhanvadia, Y. J. Mankad, A. L. Patel and S. S. Zade, *New J. Chem.*, 2018, **42**, 13565–13572.

20 H.-Y. Chen, J. Hou, A. E. Hayden, H. Yang, K. N. Houk and Y. Yang, *Adv. Mater.*, 2010, **22**, 371–375.

21 K.-T. Wong, T.-C. Chao, L.-C. Chi, Y.-Y. Chu, A. Balaiah, S.-F. Chiu, Y.-H. Liu and Y. Wang, *Org. Lett.*, 2006, **8**, 5033–5036.

22 C.-H. Chen, Y.-J. Cheng, M. Dubosc, C.-H. Hsieh, C.-C. Chu and C.-S. Hsu, *Chem. – An Asian J.*, 2010, **5**, 2483–2492.

23 Y. Wu, Z. Li, X. Guo, H. Fan, L. Huo and J. Hou, *J. Mater. Chem.*, 2012, **22**, 21362–21365.

24 Y.-J. Cheng, C.-H. Chen, T.-Y. Lin and C.-S. Hsu, *Chem. – An Asian J.*, 2012, **7**, 818–825.

25 L. Biniek, B. C. Schroeder, J. E. Donaghey, N. Yaacobi-Gross, R. S. Ashraf, Y. W. Soon, C. B. Nielsen, J. R. Durrant, T. D. Anthopoulos and I. McCulloch, *Macromolecules*, 2013, **46**, 727–735.

26 H. A. Patel, V. J. Bhanvadia, H. M. Mande, S. S. Zade and A. L. Patel, *Org. Biomol. Chem.*, 2019, **17**, 9467–9478.

27 U. H. F. Bunz, J. U. Engelhart, B. D. Lindner and M. Schaffroth, *Angew. Chem. Int. Ed. Engl.*, 2013, **52**, 3810–3821.

28 H.-Y. Chen, J. Hou, S. Zhang, Y. Liang, G. Yang, Y. Yang, L. Yu, Y. Wu and G. Li, *Nat. Photonics*, 2009, **3**, 649–653.

29 I. Osaka, T. Kakara, N. Takemura, T. Koganezawa and K. Takimiya, *J. Am. Chem. Soc.*, 2013, **135**, 8834–8837.

30 D. Zhang, L. Zhao, Y. Zhu, A. Li, C. He, H. Yu, Y. He, C. Yan, O. Goto and H. Meng, *ACS Appl. Mater. Interfaces*, 2016, **8**, 18277–18283.

31 W. Zhou, Y. Wen, L. Ma, Y. Liu and X. Zhan, *Macromolecules*, 2012, **45**, 4115–4121.

32 H. Li, F. S. Kim, G. Ren and S. A. Jenekhe, *J. Am. Chem. Soc.*, 2013, **135**, 14920–14923.

33 J. Liu, H. Zhang, H. Dong, L. Meng, L. Jiang, L. Jiang, Y. Wang, J. Yu, Y. Sun, W. Hu and A. J. Heeger, *Nat. Commun.*, 2015, **6**, 10032 (1–8).

34 C. Guo, B. Sun, J. Quinn, Z. Yan and Y. Li, *J. Mater. Chem. C*, 2014, **2**, 4289–4296.

35 T. Lei, J. H. Dou, Z. J. Ma, C. H. Yao, C. J. Liu, J. Y. Wang and J. Pei, *J. Am. Chem. Soc.*, 2012, **134**, 20025–20028.

36 W. Cui, J. Yuen and F. Wudl, *Macromolecules*, 2011, **44**, 7869–7873.

37 J. W. Rumer, S. Dai, M. Levick, L. Biniek, D. J. Procter and I. Mcculloch, *J. Polym. Sci. Part A Polym. Chem.*, 2012, **51**, 1285–1291.

38 H. Hwang, D. Khim, J. M. Yun, E. Jung, S. Y. Jang, Y. H. Jang, Y. Y. Noh and D. Y. Kim, *Adv. Funct. Mater.*, 2015, **25**, 1146–1156.

39 Y. Deng, B. Sun, Y. He, J. Quinn, C. Guo and Y. Li, *Angew. Chemie - Int. Ed.*, 2016, **55**, 3459–3462.

40 V. J. Bhanvadia, A. Choudhury, P. K. Iyer, S. S. Zade and A. L. Patel, *Polymer (Guildf).*, 2020, **210**, 123032.

41 C. Lu, H.-C. Chen, W.-T. Chuang, Y.-H. Hsu, W.-C. Chen and P.-T. Chou,

Chem. Mater., 2015, **27**, 6837–6847.

42 F. L. Kiss, B. P. Corbet, N. A. Simeth, B. L. Feringa and S. Crespi, *Photochem. Photobiol. Sci.*, 2021, **20**, 927–938.

43 J. S. Li, Y. W. Huang, Y. C. Lin, F. H. Chen, W. C. Chen and C. C. Chueh, *J. Polym. Res.*, 2021, **28**, 1–12.

44 J. Cao, X. Luo, S. Zhou, Z. Wu, Q. Zhao, H. Gu, W. Wang, Z. Zhang, K. Zhang, K. Li, J. Xu, X. Liu, B. Lu and K. Lin, *Int. J. Mol. Sci.*, 2020, **7**, 193.

45 M. Hui, S. Heng, G. Toh, P. Jin, Z. Mao, Q. Zhu and S. Xiong, *Polym. Chem.*, 2022, **11(6)**, 1–23.

46 M. Zhu, Y. Guo and Y. Liu, *Sci. China Chem.*, 2022, **65**, 1225–1264.

47 T. Lei, J. H. Dou, X. Y. Cao, J. Y. Wang and J. Pei, *J. Am. Chem. Soc.*, 2013, **135**, 12168–12171.

48 Y. Jiang, Y. Gao, H. Tian, J. Ding, D. Yan, Y. Geng and F. Wang, *Macromolecules*, 2016, **49**, 2135–2144.

49 Y. Deng, B. Sun, Y. He, J. Quinn, C. Guo and Y. Li, *Chem. Commun.*, 2015, **51**, 13515–13518.

50 Y. Cao, J.-S. Yuan, X. Zhou, X.-Y. Wang, F.-D. Zhuang, J.-Y. Wang and J. Pei, *Chem. Commun.*, 2015, **51**, 10514–10516.

51 J.-L. Li, Y.-F. Chai, W. V. Wang, Z.-F. Shi, Z.-G. Xu and H.-L. Zhang, *Chem. Commun.*, 2017, **53**, 5882–5885.

52 W. Zhang, N. Zheng, C. Wei, J. Huang, D. Gao, K. Shi, J. Xu, D. Yan, Y. Han and G. Yu, *Polym. Chem.*, 2016, **7**, 1413–1421.

53 V. Chahal, S. NIRWAN and R. Kakkar, *Med. Chem. Commun.*, 2019, **10**, 351-368.

54 M. Jha, G. M. Shelke and A. Kumar, *European J. Org. Chem.*, 2014, **2014**, 3334–3336.

55 Z. Tribak, A. Haoudi, Y. Kandri Rodi, H. Elmsellem, M. K. Skalli, Y. Ouzidan, A. Mazzah and E. M. Essassi, *Moroccan J. Chem.*, 2016, **4(4)**, 1157-1163.

56 S. Doddi, B. Ramakrishna, Y. Venkatesh and P. R. Bangal, *RSC Adv.*, 2015, **5**, 56855–56864.

57 E. V Dalessandro, H. P. Collin, L. G. L. Guimarães, M. S. Valle and J. R. J. Pliego, *J. Phys. Chem. B*, 2017, **121**, 5300–5307.

58 V. J. Bhanvadia, H. K. Machhi, S. S. Soni, S. S. Zade and A. L. Patel, *Polymer (Guildf).*, 2020, **211**, 123089.

59 V. S. Kadam, P. A. Bhatt, H. K. Machhi, S. S. Soni, S. S. Zade and A. L. Patel, *Nano Sel.*, 2020, **1**, 491–498.

60 S. Edition, W. Koch and M. C. Holthausen, *Wolfram Koch , Max C . Holthausen A Chemist ' s Guide to*, 2001, vol. 3.

61 X. Zhao, L. Qian, J. Cao, S. Yan and L. Ding, *Polym. Chem.*, 2016, **7**, 1226–1229.

62 K. K. Sonigara, Z. Shao, J. Prasad, H. K. Machhi, G. Cui, S. Pang and S. S. Soni, *Adv. Funct. Mater.*, 2020, **30**, 1–9.

63 V. S. Kadam, H. K. Machhi, S. S. Soni, S. S. Zade and A. L. Patel, *New J. Chem.*, 2022, **46**, 8601-8610.

64 M. Jha, G. M. Shelke and A. Kumar, *European J. Org. Chem.*, 2014, **2014**, 3334–3336.

65 Z. Tribak, A. Haoudi, Y. Kandri Rodi, H. Elmsellem, M. K. Skalli, Y. Ouzidan, A. Mazzah and E. Essassi, *Mor. J. Chem*, 2016, **4**, 1157–1163.